Characteristic parameters of xenon near its liquid-gas critical point

Yves Garrabos, Carole Lecoutre-Chabot

Characteristic parameters of xenon near its liquid-gas critical point

Yves Garrabos and Carole Lecoutre
Equipe du Supercritique pour l'Environnement, les Matériaux et l'Espace - Institut de Chimie de la Matière Condensée de Bordeaux - UPR 9048, Centre National de la Recherche Scientifique - Université Bordeaux I - 87, avenue du Docteur Schweitzer, F 33608 PESSAC Cedex, France
(Dated: 24 Fev 2009)

The mean crossover functions estimated from the bounded results of the Massive Renormalization scheme applied to the $\Phi^4_d(n)$ model in three dimensions ($d = 3$) and scalar order parameter ($n = 1$) are used to represent the singular behaviors of the isothermal compressibility of xenon along the critical isochore in the homogeneous domain and the vapor-liquid coexisting densities of xenon in the nonhomogenous domain. The validity range and the Ising nature of the crossover description are discussed in terms of a single scale factor whose value can be analytically estimated *beyond* the Ising-like preasymptotic domain.

PACS numbers: 64.60.Ak., 05.10.Cc., 05.70.Jk, 65.20.+w

1. INTRODUCTION

It seems now well-established that the universal features of the one-component fluids close to their vapor-liquid critical point are Ising-like in nature [1, 2], i.e., conform with the estimated universal features close to the non-trivial fixed point of the so-called $\phi^4_{d=3}(n = 1)$ model [2, 3] (d and n are the dimensions of the space and the order parameter density, respectively). The updated leading singular behaviors [4] are then governed by the universal values [5] of two independent critical exponents, while the contribution of the confluent corrections to scaling is governed by the universal lowest value $\Delta \simeq 0.502$ [5] of the confluent exponents. These Ising-like universal features only related to the contributions of two relevant scaling fields and a single irrelevant scaling field [6, 7] are strictly valid within the *Ising-like preasymptotic domain*, i.e., a domain where each complete Wegner-like expansion [8] can be approximated by its restricted (two-terms) form [9]. Such an exact Ising-like asymptotical behavior appears as the essential tool to provide accurate determination of only three amplitudes (two leading amplitudes and one confluent amplitude) that characterize each Ising-like critical fluid [7].

However, as shown by a large set of results reported in the literature, the observed crossover behavior in one-component fluids needs to use higher-order terms in the Wegner-like expansions to fit carefully the measurements performed at finite distance to the critical point. In such an *extended asymptotic domain* covered by the fitting analysis, the above three-parameter characterization of each Ising-like fluid is not easy to probe carefully. For example, the uniqueness of the temperature-like crossover parameter (noted ϑ in the following) that complement the determination of two independent leading amplitudes has never clearly been demonstrated to define the physical temperature range of validity of the three-parameter characterization. The main goal of the present paper addresses to the explicit calculation of this single crossover parameter made *beyond* the Ising-like preasymptotic domain of xenon, using the crossover functions estimated in Refs. [9] and [10].

For xenon case, a relatively complete data set of leading amplitudes exists that is precisely conform to the two-scale-factor asymptotic universality [11, 12]. We give herafter the related analytic determination of the xenon value of a scale factor (noted $\vartheta_{\mathcal{L}}$ in the following), which characterizes the singular behavior along the critical isochore. Our $\vartheta_{\mathcal{L}}$-determination maintains the conformity with the Ising-like universal features accounted for by the theoretical crossover functions calculated in the massive renormalization scheme of the $\phi^4_{d=3}(n = 1)$ model [3, 4]. We strictly avoid adjusting any xenon-dependent parameter by a minimization of fitting errors over the experimental temperature range, as initially performed in Ref. [13]. Alternatively, only using the critical coordinates of the xenon critical point, we correlate $\vartheta_{\mathcal{L}}$ to the effective values [14] of the exponent and amplitude of a pure power law defined at a well-known finite temperature distance $(T - T_c)$ to the critical temperature (T_c), largely beyond the Ising-like preasymptotic domain. We can then found $\vartheta_{\mathcal{L}}$ from the tangent envelop of any continuous function $f_P\left(\Delta\tau^* = \frac{T-T_c}{T_c}\right)$ that fit the data measurements of the singular property P over a limited temperature range $\Delta\tau^*_{min} \leq \Delta\tau^* \leq \Delta\tau^*_{max}$. To calculate each corresponding local value of $\vartheta_{\mathcal{L}}(\Delta\tau^*)$, we use as two illustrative examples, the fitting results of Guttinger and Cannell [15] for the susceptibility data and the fitting results of Narger and Balzarini [16] for the symmetrical order parameter density data. That allows us to verify the uniqueness of the $\vartheta_{\mathcal{L}}$ value and its exact matching with the Ising asymptotic value ϑ when $\Delta\tau^* \to 0$. We simultaneously estimate the upper temperature limit of the extended asymptotic domain, providing thus the complete comparison between experimental results and crossover theories in a relative temperature range covering more than four decades above or below T_c. Moreover, as expected from the definition of the master crossover functions valid for the one-component fluid subclass [10], this comparison is made *de facto* without any adjustable

parameters when four critical coordinates of xenon are known.

The paper is organized as follows. Section 2 gives a brief recall of the useful notations and definitions with the objective to obtain the three-parameter characterization of xenon within the Ising-like preasymptotic domain. The three-parameter characterization of xenon beyond the Ising-like preasymptotic domain is defined in Section 3 analyzing the crossover behavior of the correlation length and performing both related applications of the crossover functions for the isothermal compressibility case and the order parameter density case. In Appendix A, we recall the main literature sources to estimate the critical coordinates of the vapor liquid critical point of xenon. In Appendix B, we give an illustration of the analytic determination of the local value of the crossover parameter $\vartheta_{\mathcal{L}}$, based on the useful (pure power law) function $f_{\kappa_T}(\Delta\tau^*) = \Gamma_e (\Delta\tau^*)^{-\gamma_e}$ to represent the effective singular behavior of the isothermal compressibility behavior in a restricted temperature range.

2. XENON CHARACTERIZATION *WITHIN* THE ISING-LIKE PREASYMPTOTIC DOMAIN.

2.1. Description of the Ising-like preasymptotic domain

In the following we consider three singular properties along the critical isochore: the correlation length $\xi^*_{\text{expt}}(\Delta\tau^*)$ and the isothermal compressibility $\kappa^*_{T,\text{expt}}(\Delta\tau^*)$ in the homogeneous domain ($\Delta\tau^* > 0$), and the order parameter density $\Delta\tilde{\rho}_{LV,\text{expt}}(|\Delta\tau^*|)$ in the nonhomogeneous domain ($\Delta\tau^* < 0$).

$$\Delta\tau^* = \frac{T - T_c}{T_c} \tag{1}$$

is the reduced temperature distance. Within the Ising-like preasymptotic domain, the singular behaviors of the fluid properties can be approximated by the two-term restricted forms of the complete Wegner-like expansions, i.e.,

$$\xi^*_{\text{expt}}(\Delta\tau^*) = \xi^+ (\Delta\tau^*)^{-\nu} \left[1 + a^+_\xi (\Delta\tau^*)^{\Delta}\right] \tag{2}$$

$$\kappa^*_{T,\text{expt}}(\Delta\tau^*) = \Gamma^+ (\Delta\tau^*)^{-\gamma} \left[1 + a^+_\chi (\Delta\tau^*)^{\Delta}\right] \tag{3}$$

$$\Delta\tilde{\rho}_{LV,\text{expt}}(|\Delta\tau^*|) = B |\Delta\tau^*|^{\beta} \left[1 + a_M |\Delta\tau^*|^{\Delta}\right] \tag{4}$$

In Eq. (2), $\xi^*_{\text{expt}} = \frac{\xi_{\text{expt}}}{\alpha_c}$ and $\xi^+ = \frac{\xi^+_0}{\alpha_c}$, where

$$\alpha_c = \left(\frac{k_B T_c}{p_c}\right)^{\frac{1}{d}} = (\beta_c p_c)^{-\frac{1}{d}} \tag{5}$$

with $d = 3$ and

$$(\beta_c)^{-1} = k_B T_c \tag{6}$$

α_c and $(\beta_c)^{-1}$ are the length and energy units, respectively (subscript c refers to a critical parameter). p (p_c) is the pressure (critical pressure). The superscript star labels dimensionless quantities obtained only using α_c and $(\beta_c)^{-1}$ when the thermodynamic properties are normalized per particle [17–19]. On the other hand, in Eq. (4),

$$\Delta\tilde{\rho}_{LV,\text{expt}} = \frac{\rho_L - \rho_V}{2\rho_c} \tag{7}$$

is the practical (symmetrical) dimensionless form of the order parameter density. ρ_L (ρ_V) is the density of the liquid (vapor) coexisting phase, while ρ (ρ_c) is the (critical) mass density. Equation (7) introduces the dimensionless form $\tilde{\rho} = \frac{\rho}{\rho_c}$ of the (mass) density [20, 21]. Correspondingly, the dimensionless ordering field is defined as

$$\Delta\tilde{\mu} = \tilde{\mu}_\rho - \tilde{\mu}_{\rho,c} \tag{8}$$

where $\Delta\tilde{\mu}$ is also written using a practical dimensionless form $\tilde{\mu} = \frac{\mu_\rho \rho_c}{p_c}$ [20, 21] of the chemical potential. μ_ρ ($\mu_{\rho,c}$) is the (critical) chemical potential per mass unit. The subscript ρ distinguishes the thermodynamic quantities which are expressed per mass unit. The related practical dimensionless variables using critical parameters such as ρ_c and $\frac{\rho_c}{p_c}$ are then decorated by a tilde. The definition of $\tilde{\mu}_\rho$ introduces another unit $\frac{p_c}{\rho_c} \sim \left[\frac{\text{energy}}{\text{mass}}\right]$ for (specific) energy. This latter critical ratio differs from $(m_{\bar{p}}\beta_c)^{-1}$ by the factor Z_c. $m_{\bar{p}}$ is the (molecular) mass of the fluid, while the subscript $\bar{p}$ now recalls for thermodynamic quantities expressed per particle. Correlatively, the total mass unit ($M = 1$) of a one-component fluid system introduces the critical specific volume $v_{c,M=1} = \frac{1}{\rho_c}$, which differs from $v_{c,I} = \frac{k_B T_c}{p_c} = (\alpha_c)^d$, i.e., the volume of the critical interaction cell [17]. That provides alternative choice between two energy units and two length units which originate from thermodynamics normalized, either per particle, or per mass unit. However, the comparison between the two volumes reflects the extensive nature of the fluid: at critical density, the amount of matter $\frac{m_{\bar{p}}}{Z_c}$ is contained within the microscopic interaction cell of volume $v_{c,I} = (\alpha_c)^d$, which is thus filled with $\frac{1}{Z_c}$ particles. Only $v_{c,I} = (\alpha_c)^d$ takes physical meaning in terms of the short ranged molecular interactions between the $\frac{1}{Z_c}$ fluid particles, leading to the appropriate understanding of the correlation length value, measured in unit of α_c.

For $\xi^*_{\text{expt}}(\Delta\tau^*)$, $\kappa^*_{T,\text{expt}}(\Delta\tau^*)$, and $\Delta\tilde{\rho}_{LV,\text{expt}}(|\Delta\tau^*|)$, we expect to define the amplitudes of Eqs. (2) to (4) from the corresponding two-term restricted forms of, either the mean crossover functions given in Ref. [9], or the master crossover functions, as described in Ref. [10]. Therefore, among the three leading amplitudes ξ^+, Γ^+ and B, only two are fluid dependent [22], while among the three

confluent amplitudes a_ξ^+, a_χ^+, and a_M, only one is fluid dependent. Selecting for example the amplitude set [9]

$$S_{A,f} = \left\{a_\chi^+; \xi^+; \Gamma^+\right\} \tag{9}$$

to characterize each one-component fluid f, the remaining amplitudes can then be calculated using the following universal amplitude ratios and combinations

$$\left(\xi^+\right)^{-d} \frac{\Gamma^+}{B^2} = \frac{R_C}{\left(R_\xi^+\right)^d} \tag{10}$$

$$\frac{a_\xi^+}{a_\chi^+} = 0.67919 \tag{11}$$

$$\frac{a_M}{a_\chi^+} = 0.9 \tag{12}$$

with $R_C = 0.0574$ and $R_\xi^+ = 0.2696$ [5]. Now, in order to determine the values of $S_{A,Xe} = \left\{a_\chi^+; \xi^+; \Gamma^+\right\}$ for the xenon case, we apply the mean and master theoretical crossover descriptions given in Refs. [9] and [10], respectively. A *mean* crossover function valid for any three-dimensional (uniaxial) Ising-like system refers to a complete crossover function estimated in Ref. [9] (noted I in the following). A *master* crossover function only valid for any one-component fluid refers to the modification of this complete function as proposed in Ref. [10] (noted II in the following).

2.2. Asymptotic characteristic parameters of xenon

The minimal material needed to calculate all xenon amplitudes is provided by the set of four critical coordinates

$$Q_{c,a_{\bar{p}}}^{min} = \left\{T_c; p_c; v_{\bar{p},c}; \gamma_c^{'}\right\} \tag{13}$$

which localizes the xenon critical point on the phase surface of equation of state $\Phi_{a_{\bar{p}}}^p\left(p, v_{\bar{p}}, T\right) = 0$. We have fixed the value $\Lambda_{qe}^*\left(\text{xenon}\right) = 1$ (see Ref. [23] for detail) to neglect the quantum effects at the microscopic length scale. In $Q_{c,a_{\bar{p}}}^{min}$ or $\Phi_{a_{\bar{p}}}^p$, the subscript $a_{\bar{p}}$ recall for the thermodynamic description starting from the Helmholtz free energy of the xenon particle, while $v_{\bar{p}} = \frac{m_{\bar{p}}}{\rho} = \frac{1}{n}$ is the molecular volume and $\gamma_c^{'}$ is the common critical direction at the critical temperature of the critical isochoric line and the saturation pressure curve in the $p;T$ diagram. The selected critical coordinates of xenon are:

$$\begin{aligned} T_c &= 289.733\,\text{K}, \\ p_c &= 5.84007\,\text{MPa}, \\ \rho_c &= 1113\,\text{kg}\,\text{m}^{-3} \text{ or } v_{\bar{p},c} = 0.19596\,\text{nm}^3, \\ \gamma_c^{'} &= 0.1197\,\text{MPa}\,\text{K}^{-1}, \\ \text{with}\, m_{\bar{p}} &= 2.1805 \times 10^{-25}\,\text{kg}. \end{aligned} \tag{14}$$

The data sources and references are given in Appendix A. From Eqs. (14), (5) and (6), we obtain the following critical values of the energy and length units:

$$\left(\beta_c\right)^{-1} = 4.0003 \times 10^{-21}\,\text{J} \tag{15}$$

$$\alpha_c = 0.881498\,\text{nm} \tag{16}$$

The values of the scale factors Y_c and Z_c are :

$$\begin{aligned} Z_c = \frac{p_c m_{\bar{p}}}{\rho_c k_B T_c} &= 0.28602 \\ Y_c = \gamma_c^{'} \frac{T_c}{p_c} - 1 &= 4.93846 \end{aligned} \tag{17}$$

Following the results of II and Eqs. (15) to (17), the xenon values of the dimensionless amplitudes of the characteristic set $S_{A,\text{Xe}}$ are:

$$S_{A,\text{Xe}} = \left\{ \begin{array}{c} a_\chi^+ = \left(Y_c\right)^\Delta \mathcal{Z}_\chi^{1,+} = 1.23709 \\ \xi^+ = \left(Y_c\right)^{-\nu} \mathcal{Z}_\xi^+ = 0.209338 \\ \Gamma^+ = \left(Z_c\right)^{-1} \left(Y_c\right)^{-\gamma} \mathcal{Z}_\chi^+ = 0.0578238 \end{array} \right\} \tag{18}$$

where the master amplitude set

$$\mathcal{S}_A^{\{1f\}} = \left\{ \begin{array}{rl} \mathcal{Z}_\chi^{1,+} = & 0.555 \\ \mathcal{Z}_\xi^+ = & 0.5729 \\ \mathcal{Z}_\chi^+ = & 0.11975 \end{array} \right\} \tag{19}$$

characterizes the master asymptotic singular behavior of the $\{1f\}$-subclass. The notations are defined in II. The value of the dimensional amplitude ξ_0^+ is

$$\xi_0^+ = \alpha_c \xi^+ = 0.184531\,\text{nm} \tag{20}$$

In addition, Eqs. (10) to (12) lead to

$$\begin{aligned} B &= 1.46762 \\ a_\xi^+ &= 0.840217 \\ a_M &= 1.11338 \end{aligned} \tag{21}$$

which closes the amplitude definitions of Eqs. (2) to (4) for the xenon case.

Now introducing the scale factor set $S_{SC}^{\{1f\}}$ that characterizes the master $\{1f\}$-subclass:

$$\mathcal{S}_{SC}^{\{1f\}} = \left\{ \begin{array}{ll} \Theta^{\{1f\}} & = 4.288 \times 10^{-3} \\ \mathbb{L}^{\{1f\}} & = 25.585 \\ \Psi^{\{1f\}} & = 1.75505 \times 10^{-4} \end{array} \right\} \tag{22}$$

and the equations:

$$\begin{aligned} \vartheta \left(Y_c\right)^{-1} &= \Theta^{\{1f\}} \\ g_0 \alpha_c &= \mathbb{L}^{\{1f\}} \\ \psi_\rho \left(Z_c\right)^{\frac{1}{2}} &= \Psi^{\{1f\}} \end{aligned} \tag{23}$$

where α_c, Y_c and Z_c are given by Eqs. (16) and (17), we can calculate the scale factor set of xenon

$$S_{SF,\text{Xe}}^{\{MR\}} = \left\{ \begin{array}{ll} \vartheta & = 0.0211752 \\ g_0 & = 29.0245\,\text{nm}^{-1} \\ \psi_\rho & = 3.28165\,10^{-4} \end{array} \right\} \tag{24}$$

The scale factors $\Theta^{\{1f\}}$, ϑ and Y_c are defined through the following linear relations betweeen the theoretical (t), the master ($\mathcal{T}^*$), and the physical ($\Delta\tau^*$) temperature-like fields

$$t = \Theta^{\{1f\}}\mathcal{T}^* = \Theta^{\{1f\}}Y_c\Delta\tau^* = \vartheta\Delta\tau^* \tag{25}$$

when $t \to 0$, $\mathcal{T}^* = Y_c\Delta\tau^* \to 0$ and $\Delta\tau^* \to 0$, along the critical isochore (zero value of the magnetic-like fields) [3, 6]. Similarly, the scale factors $\Psi^{\{1f\}}$, ψ_ρ and Z_c are defined through the following linear relations betweeen the theoretical (h), the master ($\mathcal{H}^*$), and the physical ($\Delta\tilde{\mu}$) magnetic-like fields

$$h = \Psi^{\{1f\}}\mathcal{H}^* = \Psi^{\{1f\}}Z_c\Delta\tilde{\mu} = \psi_\rho\Delta\tilde{\mu} \tag{26}$$

when $h \to 0$, $\mathcal{H}^* = Z_c\Delta\tilde{\mu} \to 0$ and $\Delta\tilde{\mu} \to 0$, along the critical isotherm ($t = \mathcal{T}^* = \Delta\tau^* = 0$) [3, 6]. The third (dimensional) scale factor g_0 is the adjustable critical coupling constant of the Φ^4 term having a correct wave number dimension [3] to be introduced in the fitting equation

$$\ell_{\text{th}}(t) = g_0\xi_{\text{expt}}(\Delta\tau^*) \tag{27}$$

The inverse wave number $(g_0)^{-1}$ acts as the physical adjustable length in the link between the theoretical dimensionless correlation length (ℓ_{th}) and the physical correlation length (ξ_{expt}) of each one-component fluid. Then, by exchanging Eq. (27) and the following dimensionless equation

$$\ell_{\text{th}}(t) = \mathbb{L}^{\{1f\}}\xi^*_{\text{expt}}(\Delta\tau^*), \tag{28}$$

we retrieve [see Eq. (23)]

$$\mathbb{L}^{\{1f\}} = \alpha_c g_0 \tag{29}$$

$\mathbb{L}^{\{1f\}}$ links both critical length units defined for $\{t = 0; h = 0\}$ and $\{\Delta\tau^* = 0; \Delta\tilde{\mu} = 0\}$, respectively. Equations (5), (6) and (29) are guarantee for uniqueness [7] of the length and energy units in the dimensionless singular behaviors of thermodynamic and correlations functions (whatever the one-component fluid).

After all, $m_{th} \to 0$ and $\Delta\tilde{\rho} \to 0$ in the non-homogeneous domain are related by the equation

$$m_{th} = \left(\mathbb{L}^{\{1f\}}\right)^{-d}(\psi_\rho)^{-1}\Delta\tilde{\rho}_{LV,\text{expt}}, \tag{30}$$

where m_{th} is the theoretical magnetization-like order parameter. Accordingly, the theoretical susceptibility $\chi_{\text{th}}(t) = \left(\frac{\partial m_{th}}{\partial h}\right)_t$ and the experimental isothermal susceptibility $\tilde{\chi}_{T,\text{expt}}(\Delta\tau^*) = \left(\frac{\partial\Delta\tilde{\rho}}{\partial\Delta\tilde{\mu}}\right)_{\Delta\tau^*}$ for fluids, are related by the equation

$$\chi_{\text{th}}(t) = \left(\mathbb{L}^{\{1f\}}\right)^{-d}(\psi_\rho)^{-2}\kappa^*_{T,\text{expt}}(\Delta\tau^*), \tag{31}$$

with $\tilde{\chi}_{T,\text{expt}}(\Delta\tau^*) \equiv \kappa^*_{T,\text{expt}}(\Delta\tau^*)$ when $\Delta\tilde{\rho} = 0$ (see above). The (three) fitting Eqs. (28), (30) and (31) close the (three) parameter characterization of the Ising-like preasymptotic domain since they provide the unambiguous determination of ϑ, $\mathbb{L}^{\{1f\}}$ (or g_0), and ψ_ρ , and consequently, a^+_χ, ξ^+, and Γ^+. Thus, we can also retrieve the results given in Eqs. (18), using the following set of equations

$$\begin{aligned} a^+_\chi &= \vartheta^{\Delta}\mathbb{Z}^{1,+}_\chi \\ \xi^+ &= \left(\mathbb{L}^{\{1f\}}\right)^{-1}\vartheta^{-\nu}\left(\mathbb{Z}^+_\xi\right)^{-1} \\ \Gamma^+ &= \left(\mathbb{L}^{\{1f\}}\right)^{d}(\psi_\rho)^2\vartheta^{-\gamma}\left(\mathbb{Z}^+_\chi\right)^{-1} \end{aligned} \tag{32}$$

where the theoretical amplitude set (see I)

$$\mathbb{S}^{\{MR\}}_A = \left\{ \begin{array}{rl} \mathbb{Z}^{1,+}_\chi & = 8.56347 \\ \left(\mathbb{Z}^+_\xi\right)^{-1} & = 0.471474 \\ \left(\mathbb{Z}^+_\chi\right)^{-1} & = 0.269571 \end{array} \right\} \tag{33}$$

characterizes the universal asymptotic singular behavior of the $\Phi_3(1)$-class.

However, we note the top-down hierarchy of Eqs. (32) that link the amplitude set $S_A = \left\{a^+_\chi; \xi^+; \Gamma^+\right\}$ and the scale factor set $S^{\{MR\}}_{SF} = \left\{\vartheta; \mathbb{L}^{\{1f\}}(\text{or}\, g_0); \psi_\rho\right\}$ for each one-component fluid. The top equation shows that ϑ characterizes the lowest order of the fluid confluent corrections to scaling in an unequivocal manner. Then the medium equation defines the dimensionles number $\mathbb{L}^{\{1f\}}$, which relates the fluid microscopic wavelength g_0 and the fluid thermodynamic length scale α_c through Eq. (29). Finally, the bottom equation introduces the scale factor ψ_ρ of the order parameter density. ψ_ρ can be estimated using any leading amplitude chosen among the ones of the extensive singular properties, as here above Γ^+ in the isothermal compressibility case. When the dimensionles number $\mathbb{L}^{\{1f\}}$ takes its master value of Eq. (22), the fluid scale factors ϑ and ψ_ρ are well unequivocally related to the fluid scale factors Y_c and Z_c respectively, as shown by Eqs. (23) and (22).

2.3. Extension of the Ising-like preasymptotic domain of xenon

The most important result is that the value of ϑ enables the estimation of the extension $\mathcal{L}^f_{\text{PAD}}$ of the Ising-like preasymptotic domain of the one-component fluid f. In the xenon case we obtain:

$$\mathcal{L}^{\text{Xe}}_{\text{PAD}} \simeq \frac{\mathcal{L}^{\text{Ising}}_{\text{PAD}}}{\vartheta(\text{Xe})} \simeq 0.9 \times 10^{-4} \tag{34}$$

with

$$\mathcal{L}^{\text{Ising}}_{\text{PAD}} \simeq \left(\frac{0.033}{S_2}\right)^2 \cong 1.9 \times 10^{-6} \tag{35}$$

In Eq. (35), $\mathcal{L}^{\text{Ising}}_{\text{PAD}}$ corresponds to the extension of the Ising-like preasymptotic $t \leq \mathcal{L}^{\text{Ising}}_{\text{PAD}}$, with $S_2 = 22.9007$

(see I). Obviously, this important result can can be retreived from the following master extension of the Ising-like preasymtotic domain of the $\{1f\}$-subclass

$$\mathcal{L}_{\rm PAD}^{\{1f\}} = \frac{\mathcal{L}_{\rm PAD}^{\rm Ising}}{\Theta^{\{1f\}}} \cong 4.7 \times 10^{-4} \tag{36}$$

using then the relation

$$\mathcal{L}_{\rm PAD}^{\rm Xe} \simeq \frac{\mathcal{L}_{\rm PAD}^{\{1f\}}}{Y_c\left({\rm Xe}\right)} \tag{37}$$

The crucial problem to define the temperature range of validity of Eqs. (2) to (4) is solved and Eq. (34) [or (37)] provides an essential tool for analyzing experimental data.

In xenon case, the Ising-like preasymptotic domain correspond to the temperature range

$$T - T_c \lesssim T_c \mathcal{L}_{\rm PAD}^{\rm Xe} = 26\,{\rm mK} \tag{38}$$

However, in this small temperature range, the experimental control of the above three parameters characterization of xenon cannot easily performed for two main reasons:

i) accurate measurements of the singular properties are generally made in a temperature range which does not reach the Ising-like preasymptotic domain (anticipating the results of the next section);

ii) data fitting beyond the Ising-like preasymptotic domain generally use a Wegner-like expansion whose validity is questionable (see I).

As a result, the Ising-like equivalence between the three independent amplitudes of Eqs. (18) and the three independent scale factors of Eqs. (24) is generally obtained without the suitable precision. Therefore, a more appropriate analysis of the experimental results beyond the Ising-like preasymptotic domain, needs to introduce additional "scaling rules" which implicitely account for the asymptotic (three-parameter) characterization only valid inside the Ising-like preasymptotic domain. In the next section, we pay special attention to an analytic method of determination of the local value of a crossover parameter that introduces the contribution of the theoretical leading power law in conformity with the two-scale-factor universality, when it is applied beyond the Ising-like preasymptotic domain.

3. XENON CHARACTERIZATION *BEYOND* THE ISING-LIKE PREASYMPTOTIC DOMAIN

3.1. Ising-like nature of the dimensionless characteristic parameters of xenon

The description of a xenon singular property $P^*\left(\Delta\tau^*\right)$ by using a mean crossover function $F_P\left(t\right)$ (defined in I) in the reduced temperature range $\Delta\tau^* > \mathcal{L}_{\rm PAD}^{\rm Xe}$ must involve contributions of the correction-to-scaling terms higher than the first one. As a consequence, the value of ϑ introduced by the asymptotical analytic relation $t = \vartheta\Delta\tau^*$, is associated to an unknown relative temperature extension $\mathcal{L}_{\rm EAD}^{\rm Xe}$, which defines the extended asymptotic domain such as $\Delta\tau^* \leq \mathcal{L}_{\rm EAD}^{\rm Xe}$. In such a finite "intermediate" range $\mathcal{L}_{\rm PAD}^{\rm Xe} < \Delta\tau^* \leq \mathcal{L}_{\rm EAD}^{\rm Xe}$, we are not able to evaluate the effective influence of the numerous corrections neglected in the massive renormalization scheme of the $\phi_{d=3}^4\left(n=1\right)$ model (see I for details). We must solve new correlative difficulties concerning the effective number (which thus can be greater than three) and the nature (which can originate from the neglected analytical and confluent effects in the critical massive renormalization scheme) of the fluid-dependent parameters.

Therefore, in the absence of information concerning the extended asymptotic domain for an actual fluid labeled f, it was proposed [4, 10] to use the following fitting equation of $P^*\left(\Delta\tau^*\right)$:

$$P^*\left(\Delta\tau^*\right) = \mathbb{P}_{0,\mathcal{L}}^* \mathbb{Z}_P \left(\Delta\tau^*\right)^{-e_P} \Pi_P\left(t^{D(t)}\right) \tag{39}$$

where the two adjustable parameters are the prefactor $\mathbb{P}_{0,\mathcal{L}}^*$ and a single effective crossover parameter $\vartheta_{\mathcal{L}}$ introduced through the linear relation:

$$t = \vartheta_{\mathcal{L}} \Delta\tau^* \tag{40}$$

In Eq. (39), each function $\Pi_P\left(t^{D(t)}\right)$ is given in the form of a three-term product of the variable $t^{D(t)}$. The exponent function $D(t) = \frac{\Delta_{\rm MF} S_2 \sqrt{t} + \Delta}{S_2 \sqrt{t} + 1}$ is independent of P^* and express the crossover of the effective confluent exponent which varies between Δ and $\Delta_{\rm MF} = \frac{1}{2}$ in the complete range $t = \{0, \infty\}$. Among the prefactors $\mathbb{P}_{0,\mathcal{L}}^*$, only two (noted below $\mathbb{L}_{0,\mathcal{L}}^*$, $\mathbb{X}_{0,\mathcal{L}}^*$), are fluid-dependent to be conform with the two-scale-factor asymptotic universality. $\vartheta_{\mathcal{L}}$ is thus only characteristic of the extension $\mathcal{L}_{\rm EAD}^f$ of the critical crossover. For the three singular properties $P^* = \left\{\xi_{\rm expt}^*; \kappa_{T,\rm expt}^*; \Delta\tilde{\rho}_{LV,\rm expt}\right\}$ of present interest, the new fitting equations thus read:

$$\xi_{\rm expt}^*\left(\Delta\tau^*\right) = \frac{\xi_{\rm expt}\left(\Delta\tau^*\right)}{\alpha_c} = \frac{\mathbb{L}_{0,\mathcal{L}}^*}{\mathbb{Z}_\xi^+ \left(\Delta\tau^*\right)^\nu \Pi_\xi^+\left(t^{D(t)}\right)} \tag{41}$$

$$\kappa_{T,\rm expt}^*\left(\Delta\tau^*\right) = \frac{\mathbb{X}_{0,\mathcal{L}}^*}{\mathbb{Z}_\chi^+ \left(\Delta\tau^*\right)^\gamma \Pi_\chi^+\left(t^{D(t)}\right)} \tag{42}$$

$$\Delta\tilde{\rho}_{LV,\rm expt}\left(|\Delta\tau^*|\right) = \mathbb{M}_{0,\mathcal{L}}^* \mathbb{Z}_M \left(|\Delta\tau^*|\right)^\beta \Pi_M\left(|t|^{D(|t|)}\right) \tag{43}$$

where the Ising-like nature of the asymptotic universality is maintained through the following combination of the three prefactors :

$$\left(\mathbb{L}_{0,\mathcal{L}}^*\right)^{-d} \frac{\mathbb{X}_{0,\mathcal{L}}^*}{\left(\mathbb{M}_{0,\mathcal{L}}^*\right)^2} = 1, \tag{44}$$

For each fluid f, the new (three-parameter) characteristic set reads

$$S_{1CP,\mathcal{L}^f}^{\{MR\}} = \left\{\vartheta_{\mathcal{L}}; \mathbb{L}_{0,\mathcal{L}}^*; \mathbb{X}_{0,\mathcal{L}}^*\right\}, \tag{45}$$

where the subscript $1CP,\mathcal{L}^f$ recalls for the use of the single crossover parameter $\vartheta_{\mathcal{L}}$ that defines the Ising-like extended asymptotic domain $\Delta\tau^* \lesssim \mathcal{L}^f_{\rm EAD} = \frac{\mathcal{L}^{\rm Ising}_{\rm EAD}}{\vartheta_{\mathcal{L}}}$ of the fluid. The set of Eq. (45) replaces the set $S^{\{MR\}}_{SF,f} = \{\vartheta; g_0; \psi_\rho\}$ of Eq. (24), previously defined in the Ising-like preasymptotic domain.

In comparison to the previous fitting Eqs. (28), (30), and (31), the noticeable modification of Eqs. (41) to (43) appears in each leading term in which $\vartheta_{\mathcal{L}}$ is no longer involved in the asymptotic scaling part of the critical behavior expressed in terms of the physical field $\Delta\tau^*$. Moreover, $\mathbb{X}^*_{0,\mathcal{L}}$ and $\mathbb{L}^*_{0,\mathcal{L}}$ are two characteristic prefactors of f, *provided that the same length unit was used to define the dimensionless quantities of Eqs.* (41) *and* (42) [7]. Correlatively, $\vartheta_{\mathcal{L}}$ is a *pure* crossover parameter, with the same value above and below T_c, which exclusively controls the magnitude of many correction terms to scaling. In addition, $\vartheta_{\mathcal{L}}$ can also integrate some effects of the neglected terms linked to the supplementary confluent exponents, such as Δ_2 or Δ_3, accounting for practical numerical approximations such as $\Delta_2 \approx 2\Delta$ or $\Delta_3 \approx 3\Delta$. $\vartheta_{\mathcal{L}}$ can also include the analytic contributions when T replaces T_c in the energy unit or in the dimensionless form of the temperature distance to the critical temperature, and when we consider Massieu forms of the singular thermodynamic potential. For each fluid f, the determination of $\vartheta_{\mathcal{L}}$ is then effectively equivalent to the determination of $\mathcal{L}^f_{\rm EAD}$. Therefore, as suggested in Ref. [4], from fitting of the correlation length, the susceptibility, and the specific heat in the homogeneous and non homogeneous domains, and fitting of the coexisting density measurements in the non-homogeneous domain, one must verify the uniqueness of the $\vartheta_{\mathcal{L}}$ value (along the critical isochore). Considering all these properties allows a consistent test for the determination of the set $S^{\{MR\}}_{1CP,\mathcal{L}^f}$, in coherence with the basic hypotheses of the renormalization group approach at the origin of the theoretical crossover functions. To avoid this large task, first we analyze in § 3.2 the Ising-like consequences of the hypothetic existence of a single scale factor $\vartheta_{\mathcal{L}}$ for the xenon correlation length case in the homogeneous domain.

3.2. Experimental, master and universal singular behavior for the dimensionless correlation length case

The experimental precision of the correlation length measurements along the critical isochore of xenon is not sufficient to estimate accuratly the confluent corrections to scaling [24]. Accordingly, its singular behavior is often given as a pure power law [25–27] applied in a large temperature range. However, in such a large temperature range, it is also clearly established that the confluent corrections have a significant contribution to the singular behavior of thermodynamic properties of xenon, as in the isothermal compressibility and order parameter density cases [15, 16]. Therefore, the universal values of the amplitude ratios of Eqs. (11) and (12) are not accounted for correctly and some inconsistencies are introduced in the Ising-like universal features of xenon properties.

Nevertheless, using for example the Guttinger and Cannell fitting result $\xi_{\rm GC} = 0.184\,{\rm nm}\,(\Delta\tau^*)^{-0.63}\left[1 + 0.55\,(\Delta\tau^*)^{0.5}\right]$ [15], and the value $\alpha_c = 0.881508\,{\rm nm}$ of Eq. (16), we can represent the experimental singular behavior of the dimensionless correlation length $\xi^*_{\rm expt}(\Delta\tau^*) = \frac{\xi_{\rm GC}}{\alpha_c}$ in the $\xi^*;\Delta\tau^*$ diagram of Fig. 1 (see continuous blue curve labeled e) in the reduced temperature range beyond the Ising-like preasymptotic domain. Now we assume the existence of a single value of the xenon crossover parameter $\vartheta_{\mathcal{L}}$, with $t = \vartheta_{\mathcal{L}}\Delta\tau^*$, such as the curve of Eq. (41) matches exactly the Guttinger and Cannell curve in this experimental temperature range $\mathcal{L}^{\rm Xe}_{\rm PAD} = \frac{\varpi t_\Delta}{\vartheta_{\mathcal{L}}} < \Delta\tau^* \lesssim \mathcal{L}^{\rm Xe}_{\rm EAD} < \frac{t_\Delta}{\vartheta_{\mathcal{L}}}$. We will introduce the definitions of t_Δ and ϖt_Δ below. Accordingly, we have illustrated by the black segment labeled ED the experimental domain where this hypothetic situation is valid, which can be also measured in $T - T_c$ values in the upper axis of Fig. 1. Since the single value $\vartheta_{\mathcal{L}}$ is assumed known, only the additional knowledge of the prefactor $\mathbb{L}^*_{0,\mathcal{L}}$ of Eq. (41 is needed to obtain any matching with an experimental value of $\xi^*_{\rm expt}(\Delta\tau^*)$. The subscript $\mathcal{L}$ recall here for the "non-asymptotic" character of the two parameters $\vartheta_{\mathcal{L}}$ and $\mathbb{L}^*_{0,\mathcal{L}}$, i.e., for their hypothesized existence beyond the Ising-like presaymptotic domain. The latter, i.e. $T - T_c \lesssim T_c\mathcal{L}^{\rm Xe}_{\rm PAD} = 0.026\,{\rm K}$ of Eq. (38), is schematized by the dotted arrow labeled PAD(Xe) in the upper axis of Fig. 1). Selecting then the temperature distance $T - T_c = 1\,{\rm K}$ as a typical value satisfying the mandatory condition $T - T_c \gg 0.026\,{\rm K}$, we will shown below how $\vartheta_{\mathcal{L}}$ and $\mathbb{L}^*_{0,\mathcal{L}}$ are involved in the geometrical construction of the point $\rm A_e$ in Fig. 1, which corresponds to $\xi^*_{\rm expt}\left(\Delta\tau^* = 3.45\times10^{-3}\right) = \frac{\xi_{\rm expt}}{\alpha_c} \simeq 7.8$.

In the fitting Eq. (41), the $\mathbb{Z}^+_\xi\Pi^+_\xi\left(t^{D(t)}\right)$ term is provided by the theoretical crossover function (see I)

$$\ell_{th}(t) = \frac{t^{-\nu}}{\mathbb{Z}^+_\xi\Pi^+_\xi\left[t^{D(t)}\right]} \tag{46}$$

In the $\ell_{th};t$ diagram of Fig. 1, $\ell_{th}(t)$ is represented by the full red curve u in the intermediate Ising-like universal domain $\mathcal{L}^{\rm Ising}_{\rm PAD} \le t \le t_\Delta$, which corresponds to the red segment labeled ED (see also the ending vertical arrows $\mathcal{L}^{\rm Ising}_{\rm PAD}$ and t_Δ). $\mathcal{L}^{\rm Ising}_{\rm PAD}$ is given by Eq. (35). t_Δ is the theoretical crossover temperature (see I) given by

$$t_\Delta \simeq \left(\frac{1}{S_2}\right)^2 \cong 1.9\times10^{-3} \tag{47}$$

The universal function $D(t)$ takes the effective mean value $D(t_\Delta) = \frac{\Delta+\Delta_{\rm MF}}{2}$ at t_Δ. Then t_Δ characterizes the exchange between the prominent Ising-like nature of the confluent exponent due to the value $\Delta = 0.50189$

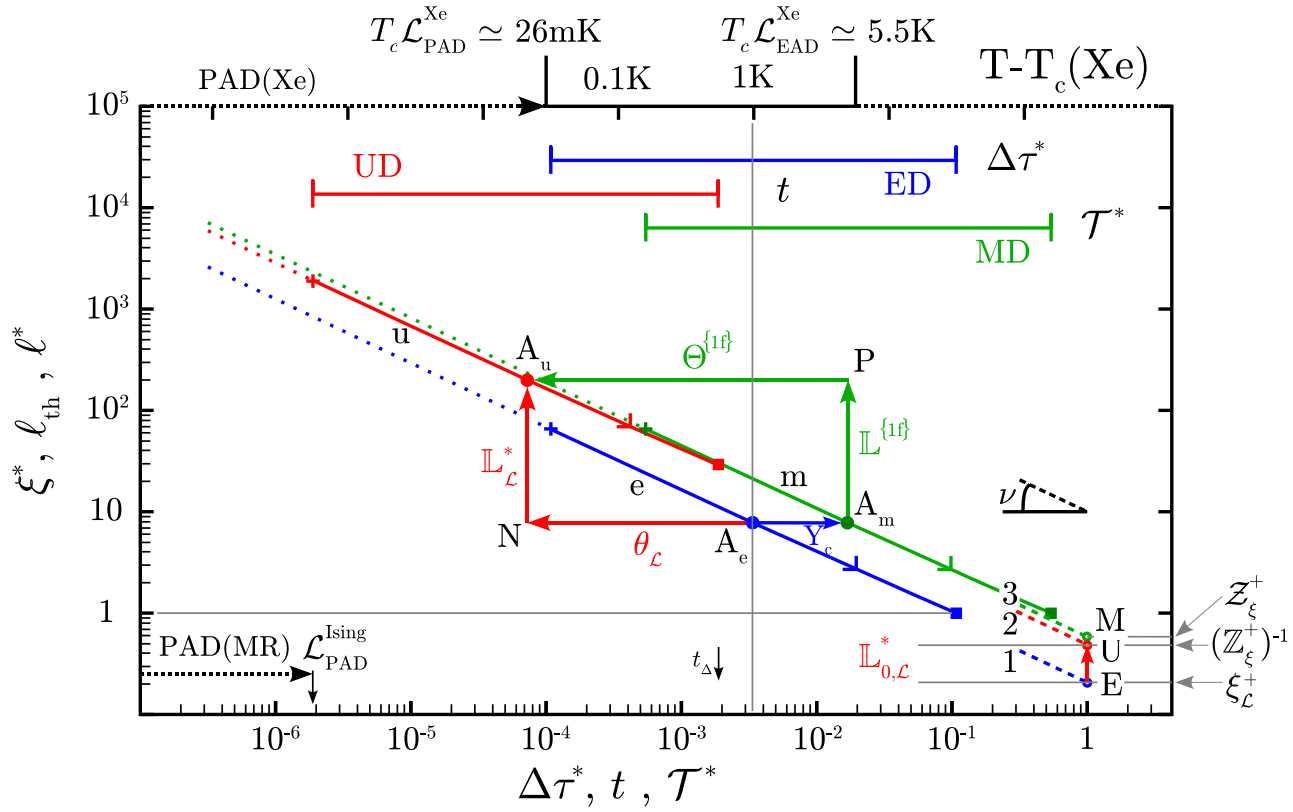

Figure 1: (Color on line) Correlation lengths as functions of their respective thermal-like fields (log-log scale). Full curves: crossover functions. Tireted lines: corresponding asymptotic power laws of slope ν. Blue, e, 1, A$_e$, E : experimental (xenon) case $\xi^*_{\rm expt}(\Delta\tau^*)$ [see Eq. (48)]. Red, u, 2, A$_u$, U : universal case $\ell_{th}(t)$ [see Eq. (46)]. Green, m, 3, A$_m$, M : master case $\ell^*(\mathcal{T}^*)$ [see Eq. (63)]. Horizontal and vertical, red $(\vartheta_{\mathcal{L}}, \mathbb{L}^*_{\mathcal{L}})$, green $(\Theta^{\{1f\}}, \mathbb{L}^{\{1f\}})$, and blue (Y_c) arrows: scale factors of Eqs. (60), (61) and (62)]. Colored circles, crosses, right corners, and squares : in same geometrical correspondance. Horizontal blue (label ED), red (UD) and green (MD) segments : intermediate crossover ranges of validity (see text). Vertical red arrow at $\Delta\tau^* = t = \mathcal{T}^* = 1$: metric parameter $\mathbb{L}^*_{0,\mathcal{L}}$ of Eq. (59). E, U, M, y-coordinates : respective prefactors parameters of Eqs. (48), (46), and (63). For other symbols and labels see text. See also Figs. 1 in Refs. [28] and [10].

approaching the non-trivial fixed point [$t \ll t_\Delta$], to its prominent mean field-like nature due to the value $\Delta_{\rm MF} = \frac{1}{2}$ approaching the Gaussian fixed point [$t \gg t_\Delta$]. As shown in I by introducing the practical relation $\mathcal{L}^{\rm Ising}_{\rm PAD} = \varpi t_\Delta$ in Eq. (35), with $\varpi \cong 10^{-3}$, we separate, either the Ising-like preasymptotic domain $t \lesssim \varpi t_\Delta$ [see arrow labelled PAD(MR) in Fig. 1], or the intermediate Ising-like crossover domain $\varpi t_\Delta < t \lesssim t_\Delta$ [see horizontal red segment labeled UD in Fig. 1]. We observe that $\ell_{\rm th}(\varpi t_\Delta) = 1916$, while $\ell_{\rm th}(t_\Delta) = 28.8$. Therefore, the Ising-like preasymptotic domain of interest in § 2 corresponds to $\ell_{\rm th} \gtrsim 1900$. Here we are concerned by approximatively two-decades of the curve u, i.e., $2000 \gtrsim \ell_{\rm th} \gtrsim 20$ and our following purpose concerns especially the point A$_u$ on this theoretical curve. Obviously, from our above hypothesized description, the experimental blue curve labeled e in Fig. 1 should be represented by the following theoretical crossover function

$$\xi^*_{\rm MR}(\Delta\tau^*) = \frac{\mathbb{L}^*_{0,\mathcal{L}}(\Delta\tau^*)^{-\nu}}{\mathbb{Z}^+_\xi \Pi^+_\xi \left[(\vartheta_{\mathcal{L}}\Delta\tau^*)^{D(\vartheta_{\mathcal{L}}\Delta\tau^*)}\right]} \qquad (48)$$

where the subscript MR recall for the massive renormalzation scheme. Equation (48) contains the implicit geometrical link between the Ising-like *theoretical* point A$_u$ and the *experimental* point A$_e$ that is only depending on $\vartheta_{\mathcal{L}}$ and $\mathbb{L}^*_{0,\mathcal{L}}$.

In Fig. 1, the relation $t = \vartheta_{\mathcal{L}}\Delta\tau^*$ corresponds to the horizontal red arrow A$_u$N (with label $\vartheta_{\mathcal{L}}$) between the x-coordinates of the points A$_e$ and A$_u$. The singleness of $\vartheta_{\mathcal{L}}$ implies the unequivocal determination of any first-amplitude $a^+_{P,\mathcal{L}}$ of confluent corrections to scaling, using the following independent equation:

$$a^+_{P,\mathcal{L}} = -(\vartheta_{\mathcal{L}})^{\Delta}\mathbb{Z}^{1,+}_P \qquad (49)$$

where $\mathbb{Z}^{1,\pm}_P$ is given in I. A single irrelevant field responsible of the confluent corrections to scaling is then only characterized by the non-asymptotic crossover parameter $\vartheta_{\mathcal{L}}$, in conformity with the universal features calculated for the lowest exponent Δ. On the other hand, for $\Delta\tau^* \to 0$, the leading amplitude of the pure asymptotic power law $\xi^*_{\rm MR}(\Delta\tau^*) = \xi^+_{\mathcal{L}}(\Delta\tau^*)^{-\nu}$ can be calculated

without reference to $\vartheta_{\mathcal{L}}$, using the equation:

$$\xi_{\mathcal{L}}^{+}=\mathbb{L}_{0,\mathcal{L}}^{*}\left(\mathbb{Z}_{\xi}^{+}\right)^{-1} \tag{50}$$

The "metric" nature of $\mathbb{L}_{0,\mathcal{L}}^{*}$ is then shown in Fig. 1 by the vertical arrow EU at $t=\Delta\tau^{*}=1$. The point E of y-coordinate $\xi_{\mathcal{L}}^{+}$ is located on the tireted blue line 1 of *experimental* pure power law $\xi_{\mathrm{MR}}^{*}\left(\Delta\tau^{*}\right)=\xi_{\mathcal{L}}^{+}\left(\Delta\tau^{*}\right)^{-\nu}$. The point U of y-coordinate $\left(\mathbb{Z}_{\xi}^{+}\right)^{-1}$ is located on the tireted red line 2 of *theoretical* pure power law $\ell_{th}\left(t\right)=\left(\mathbb{Z}_{\xi}^{+}\right)^{-1}t^{-\nu}$ (for clarity only a limited part of the lines of slope ν is represented).

However, we can also re-introduce the scale factor nature of $\vartheta_{\mathcal{L}}$ in the pure asymptotic description. The new asymptotic parameter $\mathbb{L}_{\mathcal{L}}^{*}$ is thus defined by the equation

$$\mathbb{L}_{\mathcal{L}}^{*}=\left[\mathbb{L}_{0,\mathcal{L}}^{*}\left(\vartheta_{\mathcal{L}}\right)^{\nu}\right]^{-1} \tag{51}$$

A better understanding of the role of $\mathbb{L}_{\mathcal{L}}^{*}$, needs to define simultaneously the dimensional prefactor $\mathbb{L}_{0,\mathcal{L}}$, the leading amplitude $\xi_{0,\mathcal{L}}^{+}$, and the "microscopic" wave number $g_{0,\mathcal{L}}$ of xenon by the following equations

$$\mathbb{L}_{0,\mathcal{L}}=\alpha_{c}\mathbb{L}_{0,\mathcal{L}}^{*}, \tag{52}$$

$$\xi_{0,\mathcal{L}}^{+}=\mathbb{L}_{0,\mathcal{L}}\left(\mathbb{Z}_{\xi}^{+}\right)^{-1}, \tag{53}$$

$$g_{0,\mathcal{L}}=\left(\mathbb{L}_{0,\mathcal{L}}\right)^{-1}\left(\vartheta_{\mathcal{L}}\right)^{-\nu}=\left[\alpha_{c}\mathbb{L}_{0,\mathcal{L}}^{*}\left(\vartheta_{\mathcal{L}}\right)^{\nu}\right]^{-1}. \tag{54}$$

where the subscript $\mathcal{L}$ recalls for the non-asymptotic origin of these new parameters that are $\vartheta_{\mathcal{L}}$- and $\mathbb{L}_{0,\mathcal{L}}^{*}$-dependent. Accordingly, the dimensional power law $\xi_{MR}\left(\Delta\tau^{*}\right)=\xi_{0,\mathcal{L}}^{+}\left(\Delta\tau^{*}\right)^{-\nu}$ is known, while the fitting equation (with $t=\vartheta_{\mathcal{L}}\Delta\tau^{*}$)

$$\xi_{\mathrm{MR}}\left(\Delta\tau^{*}\right)=\left(g_{0,\mathcal{L}}\right)^{-1}\ell_{th}\left(t\right) \tag{55}$$

is valid on the complete temperature range $\Delta\tau^{*}\lesssim\mathcal{L}_{\mathrm{EAD}}^{\mathrm{Xe}}$. Then, Eq. (51) can be complemented as follows

$$\mathbb{L}_{\mathcal{L}}^{*}=g_{0,\mathcal{L}}\alpha_{c}=\frac{\alpha_{c}}{\xi_{0,\mathcal{L}}^{+}}\left[\mathbb{Z}_{\xi}^{+}\left(\vartheta_{\mathcal{L}}\right)^{\nu}\right]^{-1}=\left[\xi_{\mathcal{L}}^{+}\mathbb{Z}_{\xi}^{+}\left(\vartheta_{\mathcal{L}}\right)^{\nu}\right]^{-1} \tag{56}$$

When α_{c} is known and the singleness of $\vartheta_{\mathcal{L}}$ hypothesized, the parameter $\mathbb{L}_{\mathcal{L}}^{*}$ can be substituted to the parameter $\mathbb{L}_{0,\mathcal{L}}^{*}$ by using Eq. (56). The two dimensionless parameters $\left\{\vartheta_{\mathcal{L}};\mathbb{L}_{\mathcal{L}}^{*}\right\}$ take a similar asymptotic scale factor nature to $\left\{\vartheta;\mathbb{L}^{\{1f\}}\right\}$ defined in $\mathcal{S}_{SF}$ of Eq. (24)], except that their subscript $\mathcal{L}$ recalls for the non-asymptotic hypothesized introduction of $\vartheta_{\mathcal{L}}$ and $\mathbb{L}_{0,\mathcal{L}}^{*}$, which was made considering the experimental range *beyond* the Ising-like preasymptotic domain. On other words, the extrapolated pure power laws illustrated by the tireted blue and red lines within the Ising-like preasymptotic domain are obtained without any reference to experimental measurements performed in the temperature range $T-T_{c}\leq T_{c}\mathcal{L}_{\mathrm{PAD}}^{\mathrm{Xe}}=0.026\,\mathrm{K}$. In Fig. 1, this (non-asymptotic) "scale factor" nature of $\vartheta_{\mathcal{L}}$ and $\mathbb{L}_{\mathcal{L}}^{*}$ is illustrated by the horizontal and vertical red arrows corresponding to the ratios of x- and y-coordinates of the points A_{e} and A_{u} of the curves e and u, beyond the Ising-like presymptotic domain. Obviously, in these intermediate Ising-like crossover domains, the same matching occurs for all points of the full curves e and u due to the singleness of $\vartheta_{\mathcal{L}}$ and the scale factor nature of $\vartheta_{\mathcal{L}}$ and $\mathbb{L}_{\mathcal{L}}^{*}$, as illustrated for example by the corresponding crosses, righ corners, and squares. The crosses correspond to the borderline of the Ising-like preasymptotic domains, while the right corners and squares define the conditions $\xi_{\mathrm{MR}}^{*}\simeq 2.7$ and $\xi_{\mathrm{MR}}^{*}=1$, respectively, which will be discussed below.

The missing geometrical link with our previous description of the Ising-like preasymptotic domain made in Section 2, can be provided by the master description of the correlation length of any one-component fluid [28]. As a matter of fact, if the xenon scale factor $\mathbb{L}_{\mathcal{L}}^{*}$ takes the master value $\mathbb{L}^{\{1f\}}$ of Eq. (29), thus the fitting Eq. (28) is true and the identity $\vartheta_{\mathcal{L}}\equiv\vartheta$ is valid. In that additional hypothetic situation for xenon, our previous description of the correlation length by the two-term Eq. (2) is valid within the Ising-like preasymptotic domain. The comparison with the fitting Eq. (55) obtained from measurement data beyond the Ising-like preasymptotic domain shows immediately that both non-asymptotic parameters $\vartheta_{\mathcal{L}}$ and $\left(g_{0,\mathcal{L}}\right)^{-1}$ must be unequivocally related to the critical parameters Y_{c} and α_{c} respectively, through the equations

$$\frac{\vartheta_{\mathcal{L}}}{Y_{c}}=\Theta^{\{1f\}} \tag{57}$$

$$\mathbb{L}_{\mathcal{L}}^{*}=g_{0,\mathcal{L}}\alpha_{c}\equiv\mathbb{L}^{\{1f\}} \tag{58}$$

As a correlative result, the prefactor $\mathbb{L}_{0,\mathcal{L}}^{*}$ must be also unequivocally related to the critical parameter Y_{c} through the equation (see II):

$$\begin{aligned}\mathbb{L}_{0,\mathcal{L}}^{*} &=\mathcal{Z}_{\xi}^{+}\mathbb{Z}_{\xi}^{+}\left(Y_{c}\right)^{-\nu}\\ &=\frac{1}{\left[\mathbb{L}^{\{1f\}}\times\left(\Theta^{\{1f\}}\right)^{\nu}\right]}\left(Y_{c}\right)^{-\nu}\end{aligned} \tag{59}$$

Finally, by assuming the singleness of $\vartheta_{\mathcal{L}}$ and the identity $\mathbb{L}_{\mathcal{L}}^{\{1f\}}\equiv\mathbb{L}^{\{1f\}}$, we observe that the initial hypothetic "non-asymptotic" parameters $\vartheta_{\mathcal{L}}$ and $\mathbb{L}_{0,\mathcal{L}}^{*}$ are only dependent of Y_{c}. But Y_{c} is a parameter strictly defined at the critical point that implies a pure "Ising-like" nature of the confluent corrections to scaling due to a single irrelevant fluid field. Indeed, in the scale dilatation method [19], the scale factor Y_{c} has been obtained from a physical quantity expressed in units of $\left[\frac{k_{B}}{\left(\alpha_{c}\right)^{d}}=\frac{p_{c}}{T_{c}}\right]$, which introduces a characteristic value of the entropy per particle

[29]. Y_c is then only dependent of our selected critical length unit of Eq. (5). For the correlation length measured in unit of the thermodynamic length unit α_c, the confluent corrections to scaling are governed by a single characteristic parameter of the critical interaction cell of volume $v_{c,I} = (\alpha_c)^d$, filled by $n_{c,I} = \frac{\rho_c}{k_B m_{\bar{p}}} (\alpha_c)^d = \frac{1}{Z_c}$ particles. In other words, the asymptotic master contribution of the confluent corrections for the $\{1f\}$-subclass is well due to the master properties of the critical interaction volume *only characterized by the two dimensionless numbers Y_c and Z_c* (see also II). Our present hypothetic introduction of $\vartheta_{\mathcal{L}}$ and $\mathbb{L}^*_{0,\mathcal{L}}$ to describe the xenon correlation length by Eq. (48) is then Ising-like equivalent to our previous introduction (see II) of the two dimensionless parameters $\Theta^{\{1f\}}$ and $\mathbb{L}^{\{1f\}}$ to obtain the asymptotic matching between (two-terms) master and universal crossover functions for correlation length.

However, the fact that $\Theta^{\{1f\}}$ of Eq. (23) is also a master constant for all pure fluids is already contained in our previous hypothesis that $\mathbb{L}^{\{1f\}}$ is a master constant for all pure fluids. The single needed material is the uniqueness of the length unit to express the correlation functions and the thermodynamic functions in dimensionless forms. Accordingly, the identity $\vartheta_{\mathcal{L}} \equiv \vartheta$ is strictly Ising-like equivalent to any other identity $\mathbb{L}^{\{1f\}}_{\mathcal{L}} \equiv \mathbb{L}^{\{1f\}}$, $\mathbb{L}^*_{0,\mathcal{L}} \equiv \mathbb{L}^*_0$ or $\mathbb{L}_{0,\mathcal{L}} \equiv \mathbb{L}_0$. That gives fundamental interest to recall that the following interrelated variable rescalings

$$\begin{array}{rcl} \xi^*_{\text{expt}} & \rightarrow & \ell_{\text{th}} = \mathbb{L}^{\{1f\}} \xi^*_{\text{expt}} \\ \Delta\tau^* & \rightarrow & t = \vartheta \Delta\tau^* \end{array} \tag{60}$$

$$\begin{array}{rcl} \xi^*_{\text{expt}} & \rightarrow & \ell^* \equiv \xi^*_{\text{expt}} \\ \Delta\tau^* & \rightarrow & \mathcal{T}^* = Y_c \Delta\tau^* \end{array} \tag{61}$$

$$\begin{array}{rcl} \ell^* & \rightarrow & \ell_{\text{th}} = \mathbb{L}^{\{1f\}} \ell^* \\ \mathcal{T}^* & \rightarrow & t = \Theta^{\{1f\}} \mathcal{T}^* \end{array} \tag{62}$$

provide the asymptotic theoretical matching of the experimental, universal and master singular behavior of the correlation length within the Ising-like preasymptotic domain, as described in § 2.

Therefore, accounting for Eqs. (60) to (62), Fig. 1 can be complemented by the full green curve (labeled m) of master crossover equation [28]

$$\ell^*(\mathcal{T}^*) = \frac{\mathcal{Z}^+_\xi (\mathcal{T}^*)^{-\nu}}{\Pi^+_\xi \left[\left(\Theta^{\{1f\}} \mathcal{T}^* \right)^{D\left(\Theta^{\{1f\}} \mathcal{T}^*\right)} \right]} \tag{63}$$

applied in the intermediate Ising like crossover domain of present interest (with $\Lambda^*_{qe} = 1$ in the xenon case [23]). Accordingly, we have located the point A_m of coordinates $\left\{ \mathcal{T}^* = Y_c \Delta\tau^*; \frac{\xi_{expt}(\Delta\tau^*)}{\alpha_c} \right\}$, while the tireted green line (labeled 3) corresponds to the pure power law $\ell^* = \mathcal{Z}^+_\xi (\mathcal{T}^*)^{-\nu}$. The respective master "scale factor" role of $\mathbb{L}^{\{1f\}}$ and $\Theta^{\{1f\}}$ is illustrated by the vertical and horizontal green arrows corresponding to the ratios of y- and x-coordinates of the points A_m and A_u of the curves m and u. The phsyical "scale factor" role of Y_c is given by the horizontal blue arrow corresponding to the ratios of x-coordinates of the points A_m and A_u. As previously mentioned, the same matching occurs for the corresponding crosses, righ corners, and squares of the three curves. In an equivalent manner, at $t = \mathcal{T}^* = 1$, the respective "metric" nature of the prefactors of Eqs. (46) and (63) is given by the y-coordinates of the points M and U on lines 3 and 2, respectively. The intermediate Ising-like master crossover domain corresponds to the correlation length range $70 \lesssim \ell^*(\mathcal{T}^*) \lesssim 1$ defined for the temperaturelike range such as $\frac{\varpi t_\Delta}{\Theta^{\{1f\}}} \lesssim \mathcal{T}^* \lesssim \frac{t_\Delta}{\Theta^{\{1f\}}}$ (see the green segment labeled MD in Fig. 1).

Therefore, the Ising-like equivalence between the expected identities $\vartheta_{\mathcal{L}} \equiv \vartheta$, $\mathbb{L}^{\{1f\}}_{\mathcal{L}} \equiv \mathbb{L}^{\{1f\}}$, or $\mathbb{L}^*_{0,\mathcal{L}} \equiv \mathbb{L}^*_0$ is given in Fig. 1 as a geometrical form of length equality between horizontal and vertical segments such as: $\mathrm{PA}_u = \mathrm{A}_e\mathrm{A}_m + \mathrm{NA}_e$, $\mathrm{NA}_u = \mathrm{PA}_m$, or $\mathrm{EM} = \mathrm{EU} + \mathrm{UM}$ [see Eqs. (66) to (68)]. Obviously, the results of Ref. [28] have shown that the Ising-like nature of these scale factors and prefactors is valid in the master extended temperature-like range $\mathcal{T}^* \lesssim 0.15 - 0.2$ which satisfies the condition $\ell^*(\mathcal{T}^*) \gtrsim 2.5 - 3$. The right corners in the three curves representing the different forms of the singular correlation length are representative of these Ising-like extended asymptotic domains. For the xenon case, the corresponding Ising-like extended asymptotic domain is such that $\Delta\tau^* \lesssim \mathcal{L}^{\text{Xe}}_{\text{EAD}} \simeq 2 \times 10^{-2}$, i.e., $T - T_c \lesssim T_c \mathcal{L}^{\text{Xe}}_{\text{EAD}} \simeq 5.5 - 6\,\text{K}$, as illustrated in the upper horizontal axis of Fig. 1. In the next § 3.3, we discuss the Ising-like equivalent nature of the experimental and theoretical crossovers until the critical-to-classical crossing temperatures (square symbols).

3.3. Critical-to-classical crossing temperatures

As a direct consequence of the unequivocal link between $\vartheta \equiv \vartheta_{\mathcal{L}}$ and Y_c, the identity

$$\frac{\ell_{\text{th}}(t)}{\mathbb{L}^{\{1f\}}} \equiv \frac{\xi_{\text{expt}}(\Delta\tau^*)}{\alpha_c} \tag{64}$$

occurs with $t = 0.0211752 \Delta\tau^*$ for the xenon case. Therefore, the condition $\xi_{\text{exp}}(\Delta\tau^*) \sim \alpha_c$, where the xenon correlation length is of the order of the molecular interaction range in fluids [17], corresponds to the condition $\ell_{\text{th}}(t) \sim \mathbb{L}^{\{1f\}} \simeq 25.7$. This latter value is of the same order as $\ell_{\text{th}}(t = t_\Delta) \simeq 28.8$ at the crossover temperature t_Δ. As shown in I, t_Δ is a convenient sensor to localize the t-range of the critical-to-classical crossing temperatures where the effective theoretical exponents $e_{P,e,\text{th}}(t) = -\frac{\partial Ln[F_P(t)]}{\partial Ln(t)}$ [14] crosse their mean crossover value $e_{P,\frac{1}{2}}\left(t_{e_{P,\frac{1}{2}}}\right) = \frac{e_P + e_{P,\text{MF}}}{2}$ (see Figure 4 in I). For the correlation length and susceptibility cases, $t_{\nu_{\frac{1}{2}}} \cong 3 \times 10^{-3}$

and $t_{\gamma_{\frac{1}{2}}} \cong 4 \times 10^{-3}$, respectively, with $\ell_{\rm th}\left(t_{\nu_{\frac{1}{2}}}\right) = 22.2$ and $\ell_{\rm th}\left(t_{\gamma_{\frac{1}{2}}}\right) = 18.8$. Therefore, the Ising-like prominent nature of $F_P\left(e_{P,\rm th}\right)$, defined by the equivalent conditions $\ell_{\rm th}\left(t\right) \gtrsim \mathbb{L}^{\{1f\}}$ or $e_{P,e,\rm th}\left(t\right) \subset \left\{e_P, e_{P,\frac{1}{2}}\right\}$, is similar to the Ising-like prominent nature of the confluent function $D(t)$ in the temperature-like range $t \lesssim t_\Delta$. Accordingly, the experimental condition $\xi_{\rm expt}\left(\Delta\tau^*\right) \gtrsim \alpha_c$, or the measured effective exponents such as $0.63 > \nu_e \gtrsim 0.57$ and $1.24 > \gamma_e \gtrsim 1.12$, can be well-understood as related to the Ising-like prominent nature of the crossover behavior. Therefore, Eq. (64), with $t = 0.0211752\Delta\tau^*$, provides a useful tool to analyze the singular behavior of a xenon properties expressed, either as a function of $\Delta\tau^*$ (using for example an horizontal (lower) axes), or as a function of $\ell_{\rm th}\left(t\right)$ (using for example an horizontal (upper) axes) in a same diagram. Anticipating for example the discussion of the isothermal compressibility case given in § 3.4 and Appendix C, we can immediatly undestand that the effective exponent value $\gamma_{e,\rm expt} = 1.206$ measured by Güttinger and Cannell [15] implies that the equation $\gamma_{e,\rm th}\left(t\right) = \gamma_{e,\rm expt}\left(\Delta\tau^*\right)$ is satisfied for $t \cong 9.08 \times 10^{-5}$ where $\ell_{\rm th}\left(\gamma_{e,\rm th} = 1.206\right) \cong 174.7$, leading to match the experimental correlation length value $\frac{\xi_{\rm expt}}{\alpha_c} = \frac{\ell_{\rm th}}{25.7} \cong 6.77$ at $\Delta\tau^* \cong 4.3 \times 10^{-3}$, i.e., $T - T_c \stackrel{\cong}{=} 1.25\,{\rm K}$. In Appendix B, we will confirm that the effective value $\gamma_{e,\rm expt} = 1.206$ is precisely observed in the Güttinger and Cannell experiment at this temperature distance.

More generally, the asymptotic scale factor nature of $\mathbb{L}^{\{1f\}}$ in Eq. (64) implies that the uniqueness of the critical length unit is a necessary condition for a better understanding of the extension range of the Ising-like universality. Indeed, the Ising-like asymptotic matching of the different expressions of the correlation length implies equivalent Ising-like asymptotic matching of any other forms of each singular thermodynamic property, by virtue of hyperscaling. In other words, from the hypothesis of a single crossover parameter and the use of a single length unit, all pure fluid crossover functions are "Ising-like" universal:

i) only over the temperature range where *the crossover parameter is unique;*

ii) only for a *common* dimensionless critical length $\mathbb{L}^{\{1f\}}$ of all fluids which obeys to this single parameter crossover description.

Beyond the preasymptotic domain, we can thus use an alternative facet of the Ising-like universality of each mean crossover function $F_P\left(t\right)$. Indeed, we can introduce the effective universal behavior of its local exponent $e_{P,\rm th}\left(t\right)$ to asymptotically transform each thermodynamic property $P^*\left(\Delta\tau^*\right)$ into its theoretical universal function $F_P\left(e_{P,\rm th}\right)$. Our following approach of the crossover universality beyond the preasymptotic domain illustrates this transformation in a self-consistent manner for the susceptibility case, using the universal and experimental effective amplitudes attached to the local power laws with effective exponents, as initially introduced by Kouvel and Fisher in Ref. [14] and already used in II.

3.4. Effective crossover beyond the Ising-like PAD: the compressibility case as a typical example

The local values of the effective exponent $\gamma_{e,\rm th}\left(t\right)$ and effective amplitude $\mathbb{Z}^+_{\chi,e}\left(t\right)$ can be estimated by the equations

$$\gamma_{e,\rm th}\left(t\right) = -\frac{\partial Ln\left[\chi_{\rm th}\left(t\right)\right]}{\partial Lnt} \tag{65}$$

$$\mathbb{Z}^+_{\chi,e}\left(t\right) = \frac{\chi_{\rm th}\left(t\right)}{t^{-\gamma_e}} \tag{66}$$

where $\chi_{\rm th}\left(t\right)$ is given in I. Eliminating t [then simultaneously eliminating the scale factor $\vartheta_{\mathcal{L}}$ (or ϑ), since $t = \vartheta_{\mathcal{L}}\Delta\tau^*$], the theoretical classical-to-critical crossover is characterized by a "universal" theoretical curve $\mathbb{Z}^+_{\chi,e}\left(\gamma_{e,\rm th}\right)$ over the complete range $\gamma_{\rm MF} \leq \gamma_{e,\rm th}\left(t\right) \leq \gamma$ (see the mixed red curve labeled $\Phi_3\left(1\right)$-MR in Fig. 2).

Our present interest is restricted to the Ising-like range $\gamma_{e,\rm th}\left(t\right) \geq \gamma_{\frac{1}{2}} = \frac{\gamma+\gamma_{\rm MF}}{2}$ (see § 3.3 and the corresponding Ising-like behavior defined in the upper part of Fig. 2). The theoretical Ising-like limiting point takes universal coordinates $\left\{\gamma; \left(\mathbb{Z}^+_\chi\right)^{-1}\right\}$ (upper cross in Fig. 2). The small extension $\gamma - \gamma_{e,\rm th} \lesssim \mathbb{Z}^{1,+}_\chi \Delta\left(\mathcal{L}^{\rm Ising}_{\rm PAD}\right)^\Delta \approx 0.006$ of the Ising-like preasymptotic domain is magnified in the insert of Fig. 2. On the other hand, the curve $a_{\rm T}$ corresponds to the asymptotic singular behavior of the derivative $\left(\frac{\partial\mathbb{Z}^+_{\chi,e}}{\partial\gamma_e}\right)_{\gamma_e\to\gamma}$ of equation

$$\left(\frac{\partial\mathbb{Z}^+_{\chi,e}}{\partial\gamma_e}\right)_{\gamma_{e,\rm th}\to\gamma} = \left(\mathbb{Z}^+_\chi\right)^{-1}\left\{1 + \left(\frac{\gamma-\gamma_{e,\rm th}}{\Delta|\mathbb{Z}^{1,+}_\chi|}\right)^{-\left(\frac{\gamma-\gamma_{e,\rm th}}{\Delta}\right)}\left(1 - \log\left[\frac{\gamma-\gamma_{e,\rm th}}{\Delta|\mathbb{Z}^{1,+}_\chi|}\right]\right)\left(\frac{\gamma-\gamma_{e,\rm th}}{\Delta}\right)\right\} \tag{67}$$

The vertical double arrow with label (1) indicates the logarithmic divergence of $\left(\frac{\partial\mathbb{Z}^+_{\chi,e}}{\partial\gamma_e}\right)_{\gamma_{e,th}\to\gamma}$ [see Eq. (67) and II]. We note the significant difference between the curve $a_{\rm T}$ and the curve (S) which results from "analytic" error-bar correlation between the Ising values of γ and $\left(\mathbb{Z}^+_\chi\right)^{-1}$. As a matter of fact, the curve (S) corresponds to the linearized slope $\zeta^+_{\chi,0} = \frac{\left(\mathbb{Z}^+_{\chi,\max}\right)^{-1} - \left(\mathbb{Z}^+_{\chi,\min}\right)^{-1}}{\gamma_{\min}-\gamma_{\max}} = \frac{0.007171}{0.0025875} \simeq 2.8$ between the respective bounded coordinates of points A and B (see inserted table in Fig. 2 and Ref. [4] for data sources).

Since only two parameters ($\mathbb{X}^*_{0,\mathcal{L}}$ and $\vartheta_{\mathcal{L}}$) are free in fitting Eq. (42), Fig. 2 illustrates how the adjustable (metric) prefactor $\mathbb{X}^*_{0,\mathcal{L}}$ contributes to localize the fluid

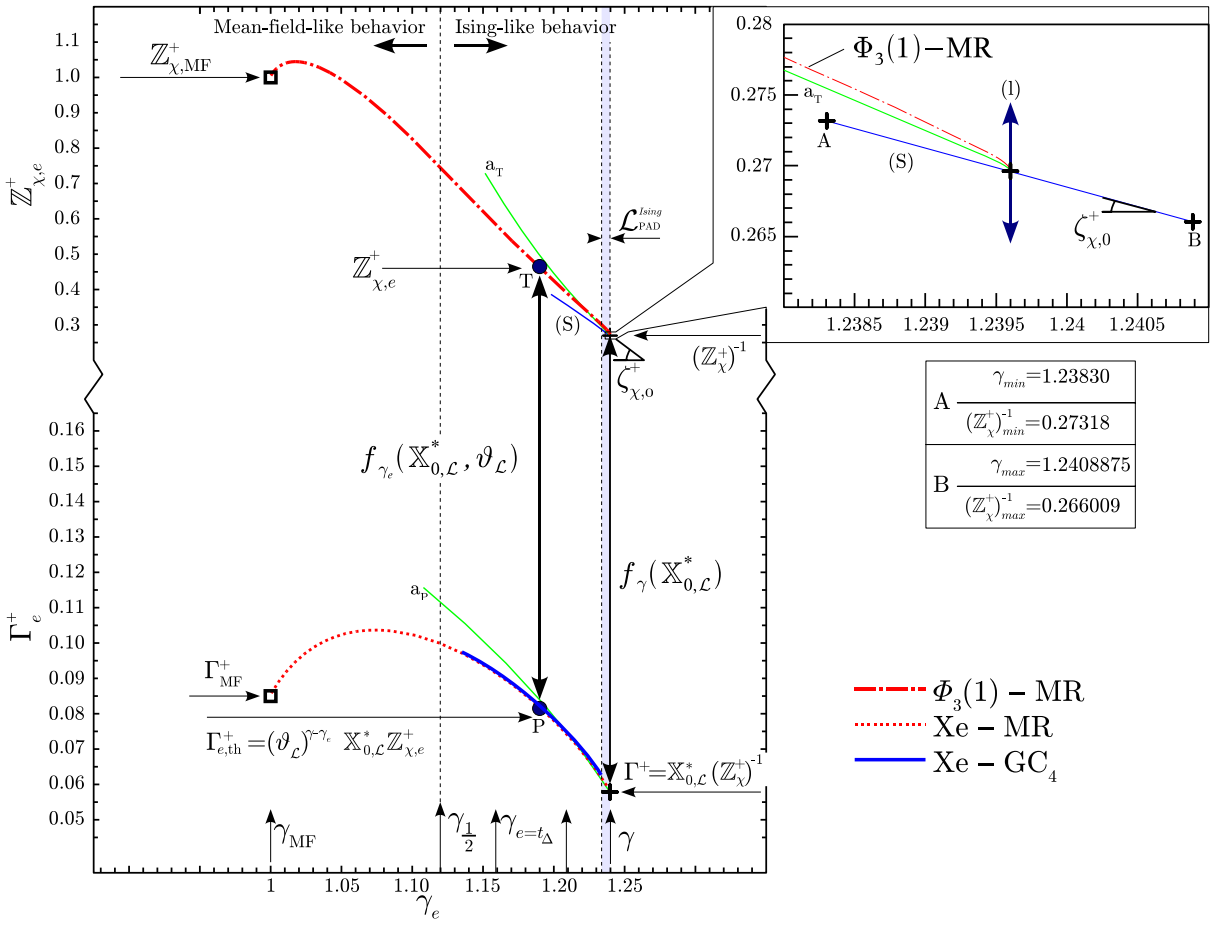

Figure 2: (Color on line) Effective dimensionless amplitudes - exponent diagram for the susceptiblity case. Upper mixed red curve labeled $\Phi_3\,(1)-\mathrm{MR}$: theoretical crossover function, see I and Eqs. (65) and (66). Lower full blue curve labeled $\mathrm{Xe}-\mathrm{GC}_4$: experimental (xenon) fitting function, see Eqs. (69) to (71) [15]. Lower dotted red curve labeled $\mathrm{Xe}-\mathrm{MR}$: theoretical-experimental matching equation of the Ising-like behavior ($\gamma_{\frac{1}{2}} < \gamma_e < \gamma$) in xenon case, see Eq. (42) and text. Vertical double arrays: two-parameter transformation $f_{\gamma_e}\left(\mathbb{X}^*_{0,\mathcal{L}},\vartheta_{\mathcal{L}}\right)$ from upper (T) and lower (P) points (circles) at constant $\gamma_e \neq \gamma$ and one-parameter transformation $f_{\gamma}\left(\mathbb{X}^*_{0,\mathcal{L}}\right)$ for the Ising-like limiting points (crosses) at $\gamma_e \equiv \gamma$. Curve labeled a_T (a_P) : effective Ising-like behavior of Eq. (67) beyond the Ising-like preasymptotic domain (experimental case). Insert : details of the singular (logarithmic) behavior (vertical double array labeled (1)) of Eq. ((67)) within the Ising-like preasymptotic domain of thickness $\mathcal{L}^{Ising}_{\mathrm{PAD}}$ (see text). For other symbols and labels see text. Se also Fig. 4 in Ref. [10].

Ising point of coordinates $\left\{\gamma;\Gamma^+=\mathbb{X}^*_{0,\mathcal{L}}\left(\mathbb{Z}^+_{\chi}\right)^{-1}\right\}$. This latter point is represented by the lower cross in Fig. 2 at the exact Ising value of the exponent for the critical xenon case. The amplitude tansformation $f_{\gamma}\left(\mathbb{X}^*_{0,\mathcal{L}}\right) \equiv \mathbb{X}^*_{0,\mathcal{L}}$ is schematized by the double array between the two crosses at the $x=\gamma$ coordinate. Therefore, the introduction of the *true* value $\Gamma^+ = \mathcal{Z}^+_{\chi}\left(Z_c\right)^{-1}\left(Y_c\right)^{-\gamma}$, as calculated in Eq. (18), fixes the value of the xenon prefactor using the following equation (see II)

$$\begin{aligned}\mathbb{X}^*_{0,\mathcal{L}} &= \mathcal{Z}^+_{\chi}\mathbb{Z}^+_{\chi}\tfrac{(Y_c)^{-\gamma}}{Z_c} \\ &= \left(\mathbb{L}^{\{1f\}}\right)^d\left(\Psi^{\{1f\}}\right)^2\left(\Theta^{\{1f\}}\right)^{-\gamma}\tfrac{(Y_c)^{-\gamma}}{Z_c}\end{aligned} \tag{68}$$

The value of $\mathbb{X}^*_{0,\mathcal{L}}$ depends on the three *asymptotic* scale factors ϑ, $\mathbb{L}^{\{1f\}}$ (or g_0), and ψ_ρ. Here $\mathbb{X}^*_{0,\mathcal{L}}$ governs the universal matching of the Ising-like limiting point and acts in a equivalent manner to $\mathbb{L}^*_{0,\mathcal{L}}$ in our previous analysis of the correlation length case. However, in this previous case, the value of $\mathbb{L}^*_{0,\mathcal{L}}$ only depended on ϑ and $\mathbb{L}^{\{1f\}}$ (or g_0), while $\mathbb{L}^{\{1f\}}$ was a master constant which

has fixed g_0 knowing α_c. Therefore, ϑ and ψ_ρ (the latter being implicitly contained in $\mathbb{X}^*_{0,\mathcal{L}}$ only, due to the extensive nature of the susceptibility) are the two fluid-dependent parameters satisfying the two-scale factor universality. In principle, the critical divergence in the initial slope at the limiting points provides the second "Ising-like constraint" to determine unambiguously the *true* asymptotic scale factor ϑ [through the relation $\vartheta = \left(\frac{a^+_\chi}{\mathbb{Z}^{1,+}_\chi}\right)^{\frac{1}{\Delta}}$ of Eq. (32), as previously mentioned in § 2.2]. Nevertheless, our previous description of the Ising-like preasymptotic domain and its above geometrical illustration underline the challenging (theoretical and experimental) difficulties to provide the exact characterization of the asymptotic scaling when a property reaches the Ising-like limiting point along a curve of *universal*, but *infinite*, slope for all the physical systems.

On the other hand, the description of the γ_e-variation in the range $\gamma - \gamma_e \gtrsim 0.015$ (i.e., in a temperature range significantly beyond the Ising-like preasymptotic domain), can be explicited in terms of universal but finite quantities. As already noted in our Introduction, that only needs to correctly fit the isothermal compressibility data by any continuous function $\kappa^*_T = f(\Delta\tau^*)$ over the restricted temperature range $\mathcal{L}^{\text{Ising}}_{\text{PAD}} \leq \Delta\tau^* \leq \Delta\tau^*_{max}$ covered by the experiments. In Appendix C for example, we will consider the useful case of an effective power law $f(\Delta\tau^*) = \Gamma^+_e (\Delta\tau^*)^{-\gamma_e}$ which was commonly used in data analysis at large distance from T_c. Hereafter we use the Güttinger and Cannell's susceptibility data fitted by the (four terms) Wegner-like expansion (labeled GC_4, see also Appendix B].

$$\kappa^*_{T,\text{expt}}(\Delta\tau^*) = \Gamma^+ (\Delta\tau^*)^{-\gamma}\left[1 + a^+_{1\chi}(\Delta\tau^*)^{\Delta} + a^+_{2\chi}(\Delta\tau^*)^{2\Delta} + a^+_{3\chi}(\Delta\tau^*)^{3\Delta}\right] \quad (69)$$

The critical exponents $\gamma = 1.241$ and $\Delta = 0.496$ [30] were fixed to the theoretical values calculated at the time by Le Guillou and Zinn-Justin from the renormalization-group approach. The values of the adjustable parameters were $\Gamma^+ = 0.0577\,(\pm 0.0001)$, $a^+_{1\chi} = 1.29\,(\pm 0.03)$, $a^+_{2\chi} = -1.55\,(\pm 0.2)$, $a^+_{3\chi} = 1.9\,(\pm 0.5)$ (the error bars quoted are one standard deviation allowing for the correlation between parameters, with an uncertainty of $\pm 0.5\,mK$ on the T_c value, see Appendix B). We can then define the following effective exponent by :

$$\gamma_{e,\text{expt}}(\Delta\tau^*) = -\frac{\partial Ln\left[\kappa^*_{T,\text{expt}}(\Delta\tau^*)\right]}{\partial Ln(\Delta\tau^*)} \quad (70)$$

and its attached effective amplitude by :

$$\Gamma^+_e(\Delta\tau^*) = \frac{\kappa^*_{T,\text{expt}}(\Delta\tau^*)}{(\Delta\tau^*)^{-\gamma_{e,exp}}} \quad (71)$$

The resulting single curve $\Gamma^+_e(\gamma_{e,\text{expt}})$ is illustrated in the lower part of Fig.2 (see the full blue curve labeled $Xe - GC_4$). The expected (two parameter) transformation $f\left(\mathbb{X}^*_{0,\mathcal{L}}, \vartheta_{\mathcal{L}}\right)$ schematized by a double array between the two points T and P on curves of well-defined *finite* slope, insures that the "xenon" theoretical curve (see the dotted red line labeled $Xe - MR$) matches the $Xe - GC_4$ curve. This transformation must contain both constraints needed to satisfy the (point) position *and* the related (tangent) direction. Therefore, the scaling nature of the matching beyond the Ising-like preasymptotic domain is significantly different in the fitting procedure which either eliminates or accounts for the contribution of the leading term. In the latter situation, we can then replace the prefactor $\mathbb{X}^*_{0,\mathcal{L}}$ by the *true* leading amplitude Γ^+, as seen below.

In the first case without contribution of the leading term *at large temperature distance*, the fit procedure based on Eq. (42) is mainly equivalent to a predominant constraint in "position" given by the following relation between the two effective exponents:

$$\gamma_{e,\text{expt}}(\Delta\tau^*) \equiv \gamma_{e,\text{th}}\left[\vartheta_{\mathcal{L}}(\Delta\tau^*)\right] \quad (72)$$

We numerically solve Eq. (72), using Güttinger and Cannell's fitting results given by Eq. (69), then providing the $\gamma_e(\Delta\tau^*)$ and $\vartheta_{\mathcal{L}}(\Delta\tau^*)$ values as a function of $\Delta\tau^*$. Both results are shown by the curve labeled GC_4 in Fig. 3a [γ_e as a function of $\Delta\tau^*$], and the curve labeled 1 in Fig. 3b [$\vartheta_{\mathcal{L}}$ as a function of $\Delta\tau^*$], respectively.

In the second case, to account for the contribution of the leading term, it is necessary to use the following scaling relation between the two effective amplitudes

$$\Gamma^+_e = (\vartheta_{\mathcal{L}})^{\gamma-\gamma_e}\,\mathbb{X}^*_{0,\mathcal{L}}\mathbb{Z}^+_{\chi,e} \quad (73)$$

Now, the transformation

$$f_{\gamma_e}\left(\mathbb{X}^*_{0,\mathcal{L}}, \vartheta_{\mathcal{L}}\right) = \mathbb{X}^*_{0,\mathcal{L}}(\vartheta_{\mathcal{L}})^{\gamma-\gamma_e} \quad (74)$$

is explicit in Eq. (73). Its takes an effective power law form of the crossover parameter $\vartheta_{\mathcal{L}}$, while the prefactor $\mathbb{X}^*_{0,\mathcal{L}}$ has (as expected above) the same value whatever the $\gamma_e\,(= \gamma_{e,\text{expt}} = \gamma_{e,\text{th}})$ value is. Equation (74) distinguishes the metric nature of $\mathbb{X}^*_{0,\mathcal{L}}$ and the scale factor nature of $\vartheta_{\mathcal{L}}$ (as in our previous analysis of the correlation length case). The both constraints in "position and direction" are correctly taken into account. Therefore, we can use the following equation

$$\Gamma^+ = \mathbb{X}^*_{0,\mathcal{L}}\left(\mathbb{Z}^+_\chi\right)^{-1} \quad (75)$$

to eliminate $\mathbb{X}^*_{0,\mathcal{L}}$ and to introduce the *true* asymptotic amplitude [which constraints the position of the Ising-like limiting point of the experimental curve in Fig. (2)]. That infers the *pure* $\vartheta_{\mathcal{L}}$-dependence of the righ-hand-side of equation

$$\frac{\Gamma^+_e}{\Gamma^+} = (\vartheta_{\mathcal{L}})^{\gamma-\gamma_e}\,\frac{\mathbb{Z}^+_{\chi,e}}{\left(\mathbb{Z}^+_\chi\right)^{-1}} \quad (76)$$

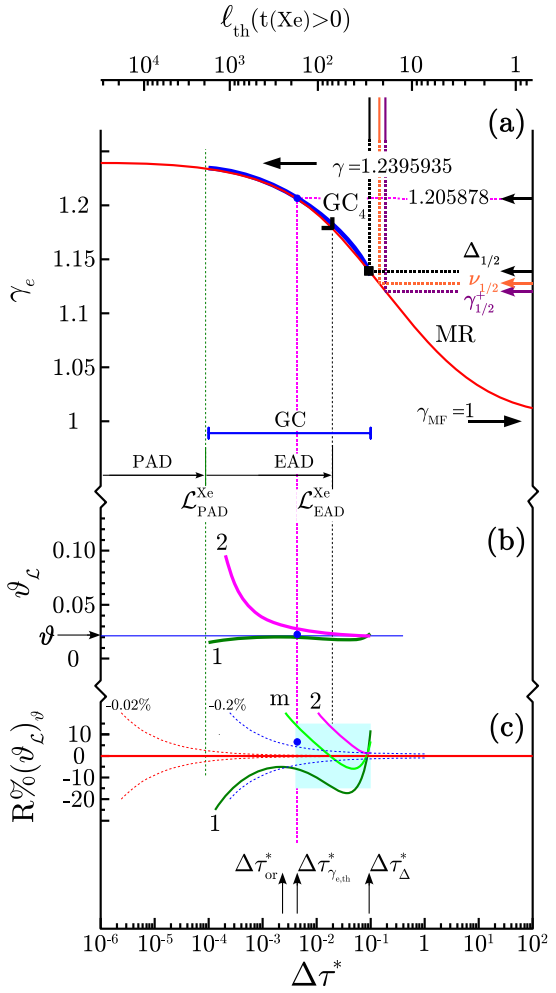

Figure 3: (Color on line) Ising-like crossover behaviors (xenon case) of γ_e (a), $\vartheta_{\mathcal{L}}$ (b), and $R\%\,(\vartheta_{\mathcal{L}})_{\vartheta} = 100\left(\frac{\vartheta_{\mathcal{L}}}{\vartheta} - 1\right)$ (c), with $\vartheta = 0.021175$ of Eq. (24), as a function of $\Delta\tau^*$ (lower horizontal axis) and $\ell_{\rm th}$ (upper horizontal axis). Part (a): black curve labeled MR: crossover function of Eq. (65); red curve labeled GC$_4$: Güttinger and Cannell [15] fitting Eq. (69); right corner and square: γ_e at temperature distances defined in Fig. 1; right side colored arrows : local values of the classical-to-critical crossing conditions defined in text. Parts (a) to (c), blue points : corresponding results at $\Delta\tau^*_{\gamma_{e,\rm th}} = 4.347\times10^{-3}$ (see Appendix B). Parts (b) and (c), curve 1: Eq. (72); curve 2: Eq. (84); Curve m: mean value of curves 1 and 2. Part (c) : residual isoclines of Eq. (B7) with $\delta\Gamma^+_e = \pm0.2\%$ and $\delta\Gamma^+_e = \pm0.02\%$ (see Appendix B). For other symbols and labels see text.

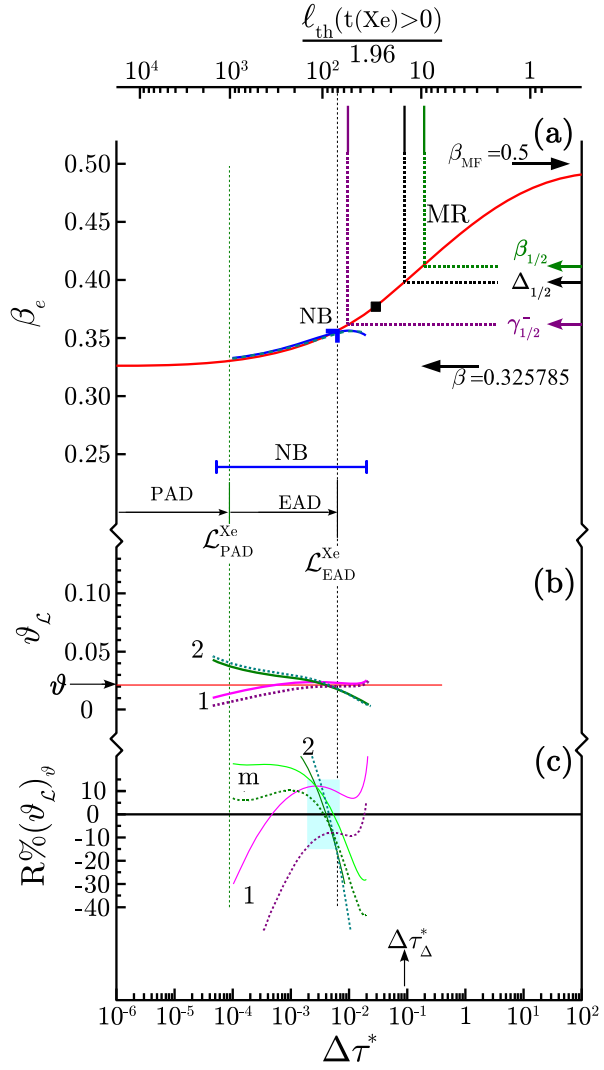

Figure 4: (Color on line) Ising-like crossover behaviors (xenon case) of β_e (a), $\vartheta_{\mathcal{L}}$ (b), and $R\%\,(\vartheta_{\mathcal{L}})_{\vartheta} = 100\left(\frac{\vartheta_{\mathcal{L}}}{\vartheta} - 1\right)$ (c), with with $\vartheta = 0.021175$ of Eq. (24), as a function of $|\Delta\tau^*|$ (lower horizontal axis) and $\ell_{\rm th}$ estimated in the non-homogeneous domain (upper horizontal axis); Part (a); curves labeled MR and NB: similar to Fig. 3 considering Narger and Balzarini fitting Eq. (78); right corner and square: values of β_e at (absolute) temperature distances defined in Fig. 1; right side colored arrows : different classical-to-critical crossing conditions defined in text. Parts (b) and (c), curve 1: Eq. (72); curve 2: Eq. (84); Curve m: mean value of curves 1 and 2. For other symbols and labels see text.

and leads to the unequivocal determination of $\vartheta_{\mathcal{L}}$ when Γ^+, γ_e and Γ^+_e are known, through the equation

$$\vartheta_{\mathcal{L}} = \left(\frac{1}{\mathbb{Z}^+_{\chi}\mathbb{Z}^+_{\chi,e}} \times \frac{\Gamma^+_e}{\Gamma^+}\right)^{\frac{1}{\gamma-\gamma_e}} \tag{77}$$

Eq. (77), applied in the extended asymptotic domain $\Delta\tau^* \lesssim \mathcal{L}^{\rm Xe}_{\rm EAD}$, has equivalent Ising-like meaning as the equation $\vartheta = \left(\frac{a^+_{\chi}}{\mathbb{Z}^{1,+}_{\chi}}\right)^{\frac{1}{\Delta}}$ [see Eq. (32)] applied within the Ising-like preasymptotic domain $\Delta\tau^* \lesssim \mathcal{L}^{\rm Xe}_{\rm PAD}$. We have numerically solve Eq. (77), with $\Gamma^+ = 0.057824$ [see Eq. (18)], by the appropriate combination between Güttinger and Cannell's fitting results and the mean crossover function for susceptibility. The resulting value $\vartheta_{\mathcal{L}}\,(\Delta\tau^*)$ corresponds to the curve labeled 2 in Figure 3b.

The available part of the curves 1 and 2 must be

restricted to the experimental temperature range illustrated by the segment labeled GC (while the calibration temperature of the Güttinger and Cannell's data is indicated by the vertical arrow labeled $\Delta\tau^*_{\rm or}$). As previously mentioned, the upper horizontal axis gives the corresponding value of the theoretical crossover function $\ell_{th}(t)$, for $t=\vartheta\Delta\tau^*>0$ and $\vartheta=0.0211752$ in xenon case. For the values of the effective exponent γ_e indicated by the black, red and brown horizontal arrows, respectivley, which correspond to the specific values $\Delta_{\frac{1}{2}}$, $\nu_{\frac{1}{2}}$, and $\gamma_{\frac{1}{2}}$, the values of $\ell_{th}(t)$ are given by the respective colored vertical arrows in the range $\ell_{th}\simeq 20-30$. The right corner and square symbols on the MR curve are indicative of the extension of the Ising-like extended asymptotic domain where $\ell_{th}\simeq 2.7\mathbb{L}^{\{1f\}}\simeq 70$ and the master crossover temperature where the correlation length is of the order of the size of the "microscopic interaction" $\ell_{th}\simeq\mathbb{L}^{\{1f\}}\simeq 25.6$, respectively (see the corresponding symbols in Fig. 1).

3.5. The order parameter density case

The above approach for the susceptibility case can be easily duplicated to the order parameter density case. In this latter case, we consider the vapor-liquid coexisting density data measured by Närger and Balzarini [16] in two different samples of xenon, which were fitted by the following (three term) Wegner-like expansion:

$$\Delta\tilde{\rho}_{LV,\rm expt}\left(|\Delta\tau^*|\right)= B\left|\Delta\tau^*\right|^{\beta}\left[1+a_{1M}\left|\Delta\tau^*\right|^{\Delta}+a_{2M}\left|\Delta\tau^*\right|^{2\Delta}\right] \tag{78}$$

For the fits, the exponents $\beta=0.327$ and $\Delta=0.5$ were held fixed. For sample No. 1, the corresponding values of the adjustable parameters are $B=1.479\,(\pm 0.011)$, $a_{1M}=1.15\,(\pm 0.19)$, $a_{2M}=-2.6\,(\pm 1.0)$ (with an uncertainty of ± 1 mK on the T_c value). This fitting result is labeled NB_{3a}. For sample No. 2, the fit results are $B=1.470\,(\pm 0.010)$, $a_{1M}=1.20\,(\pm 0.17)$, $a_{2M}=-2.8\,(\pm 1.1)$ (with an uncertainty of ± 2 mK on the T_c value), and the label is NB_{3b}.

We do not report here the complete descriptions of the effective power laws $\mathbb{Z}_{M,e}\left|t\right|^{\beta_e}$ and $B_e\left|\Delta\tau^*\right|^{\beta_e}$. We merely recall that they allow us to construct the theoretical and experimental curves of respective equations $\mathbb{Z}_{M,e}\left(\beta_e\right)$ and $B_e\left(\beta_e\right)$. The latter equations introduce the two-parameter transformation

$$f_{\beta_e}\left(\mathbb{M}^*_{0,\mathcal{L}},\vartheta_{\mathcal{L}}\right)=\mathbb{M}^*_{0,\mathcal{L}}\left(\vartheta_{\mathcal{L}}\right)^{\beta_e-\beta}, \tag{79}$$

which is similar to the one $f_{\gamma_e}\left(\mathbb{X}^*_{0,\mathcal{L}},\vartheta_{\mathcal{L}}\right)=\mathbb{X}^*_{0,\mathcal{L}}\left(\vartheta_{\mathcal{L}}\right)^{\gamma-\gamma_e}$ for the susceptibility case [see Eq. (74)]. Thus the only needed material to obtain $\vartheta_{\mathcal{L}}$ concerns the universal feature of the matching between the Ising-like limiting points at $\beta_e=\beta$. Here, the limiting transformation reads $f_{\beta}\left(\mathbb{M}^*_{0,\mathcal{L}}\right)\equiv\mathbb{M}^*_{0,\mathcal{L}}$. The corresponding value of the xenon prefactor $\mathbb{M}^*_{0,\mathcal{L}}$ can be obtained using the following relations (see II)

$$\begin{aligned}\mathbb{M}^*_{0,\mathcal{L}}&=\tfrac{\mathbb{Z}_M}{\mathcal{Z}_M}\tfrac{\left(Y_c\right)^{\beta}}{\left(Z_c\right)^{\frac{1}{2}}}\\&=\left(\mathbb{L}^{\{1f\}}\right)^{d}\Psi^{\{1f\}}\left(\Theta^{\{1f\}}\right)^{\beta}\tfrac{\left(Y_c\right)^{\beta}}{\left(Z_c\right)^{\frac{1}{2}}}\end{aligned} \tag{80}$$

which satisfy the two-scale factor universality through its analytical combination [see Eq. (44)] with $\mathbb{L}^*_{0,\mathcal{L}}$ of Eq. (59) and $\mathbb{X}^*_{0,\mathcal{L}}$ of Eq. (68). The implicit asymptotic dependence of the scale factors ϑ and ψ_ρ is thus properly accounted for, i.e., in conformity with the two-scale factor universality of pure scaling. In that pure power law asymptotical scheme, the introduction of the true value $B=\mathcal{Z}_M\left(Z_c\right)^{-\frac{1}{2}}\left(Y_c\right)^{\beta}$ to replace the prefactor $\mathbb{M}^*_{0,\mathcal{L}}=\frac{B}{\mathbb{Z}_M}$ complements our previous introduction of $\Gamma^+=\mathcal{Z}^+_{\chi}\left(Z_c\right)^{-1}\left(Y_c\right)^{-\gamma}$ to replace the prefactor $\mathbb{X}^*_{0,\mathcal{L}}=\Gamma^+\mathbb{Z}^+_{\chi}$ [see Eq. (75)]. We can also retrieve these amplitudes using the following equations

$$\Gamma^+=\left(\mathbb{L}^{\{1f\}}\right)^{d}\left(\mathbb{Z}^+_{\chi}\right)^{-1}\left(\psi_\rho\right)^2\vartheta^{-\gamma} \tag{81}$$

$$B=\left(\mathbb{L}^{\{1f\}}\right)^{d}\mathbb{Z}_M\psi_\rho\vartheta^{\beta} \tag{82}$$

Adding the fact that the prefactor $\mathbb{L}^*_{0,\mathcal{L}}$ leads to $\xi^+=\left(\mathbb{L}^{\{1f\}}\right)^{-1}\left(\mathbb{Z}^+_{\xi}\right)^{-1}\vartheta^{-\nu}$, we can easily verify the validity of the Ising-like universal value of the amplitude combinations of Eq. (10). Accordingly, we can formulate two matching equations for β_e and $\vartheta_{\mathcal{L}}$, similar to the ones for γ_e [see Eq. (72)] and $\vartheta_{\mathcal{L}}$ [see Eq. (77)]. In the first case using the single constraint in "position", we numerically solve the following equation between the two effective exponents:

$$\beta_{e,\rm expt}\left(|\Delta\tau^*|\right)\equiv\beta_{e,\rm th}\left[\vartheta_{\mathcal{L}}\left(|\Delta\tau^*|\right)\right] \tag{83}$$

The resulting curves $\beta_e\left[\left(|\Delta\tau^*|\right)\right]$ and $\vartheta_{\mathcal{L}}\left(|\Delta\tau^*|\right)$ are reported in Figs. 4(a) (with the label NB_3) and (b) (with the label 1), respectively (the case NB_{3a} corresponds to the full line, while the case NB_{3b} corresponds to the dashed line). In the second case using both constraints in "direction and position", the *pure* $\vartheta_{\mathcal{L}}$-dependence is obtained solving numerically the equation

$$\vartheta_{\mathcal{L}}=\left(\frac{\mathbb{Z}_M}{\mathbb{Z}_{M,e}}\times\frac{B_e}{B}\right)^{\frac{1}{\beta_e-\beta}} \tag{84}$$

The curves $\vartheta_{\mathcal{L}}\left(|\Delta\tau^*|\right)$ of Eq. (77) are labeled 2 in Fig. 4(b) (with a full line for the NB_{3a} case and a dashed line for the NB_{3b} case). Then the parts (a) and (b) of Fig. 4 for the order parameter density case are similar to the ones of Fig. 3 for the isothermal compressibility case. In Fig. 4, the available (experimental) temperature range is also illustrated by a segment (here labeled NB).

As the theoretical crossover function of the correlation length in the nonhomogeneous domain is not given in Ref. [4], we have used the realistic approximation $\ell_{th}\left(t<0\right)=\frac{\ell_{th}(t>0)}{1.96}$ to label the upper horizontal axis of Fig. 4. For the values of the effective exponent β_e indicated by the black, red and brown horizontal arrows, respectively, which correspond to $\Delta_{\frac{1}{2}}$, $\beta_{\frac{1}{2}}$ (order parameter density case), and $\gamma_{\frac{1}{2}}^{-}$ (susceptibility case in the nonhomogenous region labeled with the minus superscript), the values of $\ell_{th}\left(t\right)$ are given by the respective colored vertical arrows in the range $\ell_{th}\simeq 10-60$. As in previous Fig. 3, the right corner and square symbols on the MR curve are indicative of the extension of the Ising-like extended asymptotic domain where $\ell_{th}\simeq 2.7\mathbb{L}^{\{1f\}}\simeq 70$ and the master crossover temperature where the correlation length is of the order of the size of the "microscopic interaction" $\ell_{th}\simeq\mathbb{L}^{\{1f\}}\simeq 25.6$, respectively (see the corresponding symbols in Fig. 1). Here we observe that the crossing temperature for the susceptibility case is slightly greater than the extension temperature of the Ising-like extended asymptotic domain.

3.6. Comparison between $\vartheta_{\mathcal{L}}$ and ϑ

The relative comparison between $\vartheta_{\mathcal{L}}$ and ϑ values of xenon is made in parts (c) of Figs. 3 and 4, using the residuals $R\%\left(\vartheta_{\mathcal{L}}\right)_{\vartheta}=100\left(\frac{\vartheta_{\mathcal{L}}}{\vartheta}-1\right)$ (expressed in %). The reference is the Ising-like asymptotic value $\vartheta=0.0211752$ of Eq. (18). In each figure the residuals refer to $\vartheta_{\mathcal{L}}$ obtained as a local numerical solution of Eqs. (72) and (83) (curves labeled 1) and Eqs. (77) and (84) (curves labeled 2) respectively. The curves labeled m correspond to the respective local mean value between curves 1 and 2. For both properties, the $\vartheta_{\mathcal{L}}$-changes are given as a function of $\Delta\tau^{*}$ within the experimental temperature range. In the range $\Delta\tau^{*}<10^{-2}$, a noticeable increase of the residuals is observed approaching the critical temperature. That reflects the difference between the Ising values of the critical exponent ($\gamma=1.241$, $\beta=0.327$) used in experimental fittings and the ones ($\gamma=1.2395935$, $\beta=0.3257845$) used in the massive renormalization scheme. The abrupt increase of the residuals at large temperature range [i.e., $\Delta\tau^{*}>10^{-1}$ in Fig. 3(c) and $\Delta\tau^{*}>2\times10^{-2}$ in Fig. 4(c)] is visible (especially for curves 1). That corresponds to the upper limit of the fitting agreement using a single crossover parameter. The expected identity $\vartheta\equiv\vartheta_{\mathcal{L}}$ in xenon case, is here observed in the green area on each figure. These underlined areas correspond to an error-bar of $\pm15\%$ observed for the restricted temperature ranges $1.5\times10^{-2}\lesssim\Delta\tau^{*}\lesssim10^{-1}$ in Fig. 3(c) and $2\times10^{-3}\lesssim\Delta\tau^{*}\lesssim7\times10^{-3}$ in Fig. 4(c), which is especially narrowed in the order parameter density case. Such large values of $\Delta\tau^{*}$ are at least one and a half order of magnitude larger than the extension of the Ising-like preasymptotic domain defined by Eq. (34). The scaling Ising-like nature of Eqs. (77) and (84) is well-accounted for. Moreover, as clearly visible on both figures, the condition $\mathcal{L}_{\mathrm{EAD}}^{\mathrm{Xe}}<\Delta\tau_{\triangle}^{*}$ demonstrates the Ising-like nature of the extended asymptotic domain for critical xenon.

Such a temperature range where the exponent differences $\gamma-\gamma_e$ and $\beta_e-\beta$ reach significant values (i.e. $\gtrsim 0.02$), was largely investigated in the seventies [31], when the scaling approach of the fluid universality was based on the effective "universal" values of the critical exponents [as for example $\gamma_{e,\mathrm{EOS}}=1.19$, and $\beta_{e,\mathrm{EOS}}=0.355$ [21, 31] involved in effective rescaled formulation of a parametric equation of state]. In that effective form of the universal features observed at finite distance of the critical point, the Ising-like nature of the fluid f was then accounted for by introducing only two adjustable parameters in the equation of state. The number of fluid-dependent parameters was then conforms to our present analysis in the intermediate temperature range $\mathcal{L}_{\mathrm{PAD}}^{f}\leq\Delta\tau^{*}\leq\Delta\tau_{\Delta}^{*}$. However, the main reason to explain this result is not the two-scale factor universality but the uniqueness of the scale factor which characterizes the single irrelevant scaling field. Indeed, for the isothermal compressibility case in the homogeneous domain, we will show in Appendix B that the useful power law function $f_{\kappa_T}\left(\Delta\tau^{*}\right)=\Gamma_{e}^{+}\left(\Delta\tau^{*}\right)^{-\gamma_e}$ defined for $\Delta\tau_{min}^{*}\leq\Delta\tau^{*}\leq\Delta\tau_{max}^{*}$ can be revisited to provide the local slope of the crossover function which matches the effective slope γ_e at a single temperature-like value $t\left(\gamma_e\right)=\vartheta_{\mathcal{L}}\Delta\tau^{*}\left(\gamma_e\right)$. Γ^{+} being known [see Eq. (18)], by using Eq. (76) or (77) we obtain an unequivocal relation between Γ_{e}^{+} and $\vartheta_{\mathcal{L}}$. In Fig. 5 of Appendix B we have illustrated this local behavior corresponding to $\gamma_{e,\mathrm{fit}}=1.205879$, thanks to the high relative precision of the Güttinger and Cannell measurements between $\Delta\tau_{min}^{*}=9.115\times10^{-4}$ and $\Delta\tau_{max}^{*}=1.95\times10^{-2}$ (i.e., $0.26\,\mathrm{K}\leq T-T_c\leq5.65\,\mathrm{K}$). In Fig. 3(a), the effective slope $\gamma_{e,\mathrm{fit}}=1.205879$ should be observed at $\Delta\tau_{\gamma_{e,th}=\gamma_{e,\mathrm{fit}}}^{*}=4.347\times10^{-3}$ (see the vertical dotted pink line), while the values of $\vartheta_{\mathcal{L}}=\vartheta_{e,\mathrm{cor}}=0.022556$ [see Eq. (B3)] and $R\%\left(\vartheta_{e,\mathrm{cor}}\right)_{\vartheta}=+6.5\%$ [see Eq. (B7)] are represented by the full blue points in parts (b) and (c) of Fig. 3, respectively.

More generally, the effective non asymptotic form of any parametric equation of state with only two-fluid dependent parameters can be used to provide the local approximation of the crossover functions for each value of the effective exponent. The only needed Ising-like condition is that the correlation length satisfies the condition $\ell_{\mathrm{th}}\gtrsim70\simeq2.7\mathbb{L}^{\{1f\}}$, i.e., $\frac{\xi_{\mathrm{expt}}}{\alpha_c}\gtrsim2.5-3$, as analyzed in Refs. [28, 32–34].

4. CONCLUSION

Using xenon as a standard critical fluid, and the mean crossover functions for both the susceptibility in the homogeneous domain and the order parameter density in the nonhomogeneous domain as illustrative examples, we

have estimated the values of the fluid-dependent parameters which are compatible with the universal features predicted by the massive renormalization scheme. A special mention for the three (dimensionless) parameter characterization *within* the Ising-like preasymptotic domain was given only using a four parameter localisation of the xenon critical point.

We have shown that, when T_c and α_c are known, the mean crossover functions take a convenient explicit form to determine analytically a single crossover parameter $\vartheta_{\mathcal{L}}$ in a temperature range *beyond* the Ising-like preasymptotic domain. We have also clearly shown that the value of this crossover parameter is entirely governed by the data measurements at the largest distance to the critical point. The Ising-like nature of this crossover parameter is then revealed using the dimensionless master value of a single characteristic length. Finally, the magnitude of the resulting deviations and the range of temperature where these deviations become significant to invalidate the uniqueness of the crossover parameter are exactly accounted for.

From this Ising-like standard situation provided by critical xenon, the real extension and amplitude of the singular behavior of the fluid properties can be estimated for any one-component fluid for which the vapor-liquid critical point is localized in the pVT phase surface, thanks to the use of the master crossover functions given in II.

Appendix A: XENON CRITICAL COORDINATES

The xenon critical temperature was fixed to the value $T_c = 289.733 \pm 0.002\,\mathrm{K}$ recently recommended by Gillis et al [26, 27] from their critical temperature determination of the stirred xenon filling its acoustic resonator cell submitted to a ramp of temperature downward (in this experiment the absolute temperature precision is $\pm 15\,\mathrm{mK}$ from reference to the ITS-90 temperature scale). This value agrees with the two respective values $T_c = 289.731 \pm 0.0053\,\mathrm{K}$ and $T_c = 289.734 \pm 0.003\,\mathrm{K}$ measured (with an absolute precision of $\pm 50\,\mathrm{mK}$) by Berg and al [25] from observation of the vapor-liquid meniscus appearance and disappearance in the "Critical Viscosity of Xenon (CVX)" experiment. These central values, and their relative uncertainties essentially due to the thermostat temperature control, compare well with $T_c = 289.740 \pm 0.003\,\mathrm{K}$ obtained by Schneider et al from pVT measurements [35] and density measurements of coexisting liquid and vapor phases [36]. This latter value was generally used as a xenon critical temperature in previous review analyses [17, 20, 21] using the ITS-68 temperature scale. Indeed, the agreement was noticeable with $T_c = 289.747 \pm 0.010\,\mathrm{K}$ obtained by Cannell et al [37] from measurements of Brillouin spectrum, and $T_c = 289.736 \pm 0.002\,\mathrm{K}$ obtained by Smith et al [38] from light scattering intensity measurements. However, the Gillis et al's central value disagrees with some other values of similar relative precision (as for example: $T_c = 289.765 \pm 0.005\,K$ from Baidakov et al's [39, 40]; $T_c = 289.790 \pm 0.001\,\mathrm{K}$ from Güttinger and Cannell [15]; $T_c = 289.752 \pm 0.001\,K$ and $T_c = 289.789 \pm 0.002\,K$ from Balzarini et al's [16]).

Our calculated critical pressure $p_c = 5.84007 \pm 0.00050\,\mathrm{MPa}$ accounts for thermodynamic continuity on pressure measurements crossing the critical temperature along the critical isochore. In such a calculation (see Ref. [41] for details), the Habgood and Schneider's isotherm $p(\rho)$ at $(T_c)_{HS} = (273.15 + 16.59)\,K$ was used as the critical isotherm of xenon to estimate our above value of the critical pressure.

Our selected value of $\rho_c = 1113\,\mathrm{kg\,m^{-3}}$ has an uncertainty of $\pm 5\,\mathrm{kg\,m^{-3}}$ ($\sim \pm 0.5\%$), which accounts for the ρ_c values of Schneider et al's ($\rho_c = 1105 \pm n.a.\,\mathrm{kg\,m^{-3}}$ and $\rho_c = 1099 \pm n.a.\,\mathrm{kg\,m^{-3}}$) [35, 36], Cornfeld and Carr's ($\rho_c = 1111.2^{+1.9}_{-3.4}\,\mathrm{kg\,m^{-3}}$ for three different estimations) [42], Baidakov et al's ($\rho_c = 1112.8 \pm n.a.\,\mathrm{kg\,m^{-3}}$) [39], and Balzarini et al's ($\rho_c = 1099 \pm n.a.\,\mathrm{kg\,m^{-3}}$ [43], $\rho_c = 1116.0 \pm 1.7\,\mathrm{kg\,m^{-3}}$ and $\rho_c = 1114.7 \pm 1.7\,\mathrm{kg\,m^{-3}}$ [16]).

The value $\gamma_c^{'} = 0.1197 \pm 0.0006\,\mathrm{MPa\,K^{-1}}$ ($\sim \pm 0.5\%$) was recently estimated [41] from the joint analysis of the pVT measurements of Habgood and Schneider [35] and Michels et al [44], to account for the small differences on the critical density values. As a matter of fact, in spite of numerous values reported in the seventies literature, the determination of this finite critical derivative was never accurately analysed in xenon case [17]. We recall that, at the late sixties, the knowledge of the derivative $\left(\frac{\partial p}{\partial T}\right)_\rho$ in the vicinity of the critical point was mandatory needed when the objectives were to define the scaled forms of the equation of state (see Refs. [45–50]) and to test their related computations of the thermophysical property singularities (since the dimensionless quantity $\frac{T}{p_c}\left(\frac{\partial p}{\partial T}\right)_{\rho_c}$ appears in many thermodynamic relations). In xenon case, the dimensionless value $\frac{T_c}{p_c}\gamma_c^{'} = 6.02$ was initialy obtained by Vicentini-Misssoni et al [47] from their fitting of the pVT measurements of Habgood and Schneider (with $p_c = 5.83\,\mathrm{MPa}$, $T_c = 289.75\,K$, and $\rho_c = 1110\,kg\,m^{-3}$, as xenon critical coordinates). The related uncertainty on the dimensional value $\gamma_c^{'} = 0.1211\,\mathrm{MPa\,K^{-1}}$ was not given, in spite of the fact that this value was higher ($\sim +1.8\%$) than the one $\gamma_c^{'} = 0.1189\,\mathrm{MPa\,K^{-1}}$ initially found by Habgood and Schneider from a self-consistent analysis of the derivative $\left(\frac{\partial p}{\partial T}\right)_\rho$ graphically deduced from their pVT measurements. Subsequently, several published values [such as $\gamma_c^{'} = 0.11916\,\mathrm{MPa\,K^{-1}}$ from Cannell and Benedek [37], $\gamma_c^{'} = 0.12027\,\mathrm{MPa\,K^{-1}}$ from Smith et al [38], $\gamma_c^{'} = 0.1196\,\mathrm{MPa\,K^{-1}}$ from Swinney and Henry [51], $\gamma_c^{'} = 0.1192 \pm 0.0012\,\mathrm{MPa\,K^{-1}}$ from Garrabos [17]] were obtained from these Habgood and Schneider's data source and same xenon critical parameters. On the other hand, Badaikov et al have determined two values,

$\gamma_c^{'} = 0.1865\,\mathrm{MPa\,K^{-1}}$ [39], and $\gamma_c^{'} = 0.1977\,\mathrm{MPa\,K^{-1}}$ [40], from their vapor pressure data below T_c. Berg and al [25, 52] have used the dimensionless value $\frac{T_c}{p_c}\gamma_c^{'} = 5.65$ (with an uncertainty of $\pm 2.9\%$), in their viscosity data analysis of the CVX experiment with $\rho_c = 1110\,kg\,m^{-3}$. Their related value $\gamma_c^{'} = 0.113686\,\mathrm{MPa\,K^{-1}}$ is significantly lower ($\simeq -5.\%$) than a selected value in the range $\gamma_c^{'} = 0.1195 - 0.1197\,\mathrm{MPa\,K^{-1}}$. More recently, Gillis et al, selecting the "highest" value $\rho_c = 1116\,kg\,m^{-3}$ of the critical density, have used the dimensionless value $\frac{T_c}{p_c}\gamma_c^{'} = 5.9253$ calculated by Swinney and Henry for the "presumable" critical isochore at $\rho = 1110\,kg\,m^{-3}$, attributing then an uncertainty of 0.2% on the corresponding value $\gamma_c^{'} = 0.1195\,\mathrm{MPa\,K^{-1}}$. Therefore, still today, the largest uncertainty in the xenon critical coordinates of Eq. (14) comes from the determination of $\gamma_c^{'}$, which is then dependent of the selected value for the critical density. In the future, a better estimation of $\gamma_c^{'}$ needs that the two derivatives $\left(\frac{\partial p}{\partial T}\right)_\rho$ and $\left[\frac{\partial}{\partial \rho}\left(\frac{\partial p}{\partial T}\right)_\rho\right]_T$ to be determined simultaneously in the vicinity of the critical point in order to account correctly for the contribution of the relative uncertainty in the ρ_c value.

Two conclusive remarks can be formulated.

(i) The values of Eq. (14) are in remarkable agreement with the ones defined by Gillis et al [26] in their recent analysis of the sound attenuation (in the frequency range $100 < f\,(\mathrm{Hz}) < 7500$) by thermoacoustic layers between solid surfaces and xenon at critical density.

(ii) The values of Eq. (14) are of basic interest using the scaled forms of the equation of state of xenon [45–50, 53, 54]. Especially in the linear-model parametric equation of state [48, 50] and the Ho and Lister's [48] restricted cubic model of the equation of state, the singular behavior of each fluid is characterized by only two dimensionless numbers (k and a in standard notations). Now we are able [10] to estimate the xenon parameters k and a only from our above values of the critical point coordinates. However, we recall that these parametric models are not quantitatively exact in regards to the Ising-like universal combinations of the leading amplitudes [55].

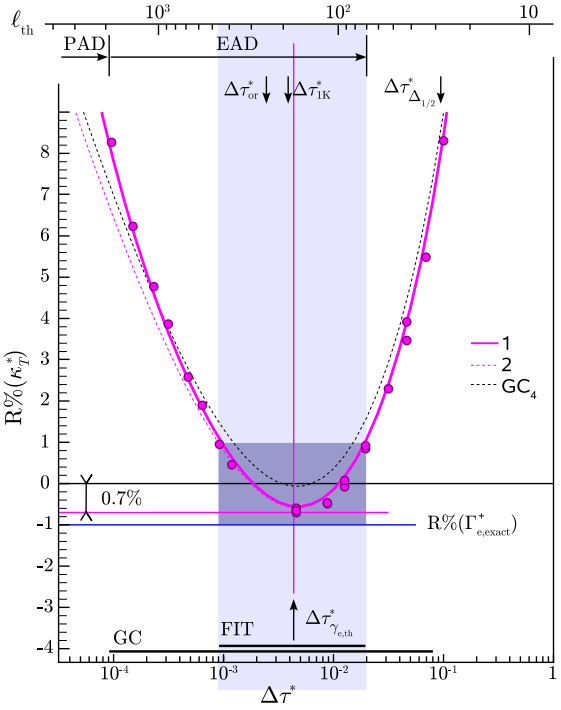

Figure 5: (Color on line) Residuals $R\%\,(\kappa_T^*)$ (expressed in %) of κ_T^* data from $\kappa^*_{T,\rm fit} = 0.07551466\,(\Delta\tau^*)^{-1.205879}$. Segment labeled FIT and underlined gray area: restricted $\Delta\tau^*$ range and 1% error-bar of the fit (see text). Segment labeled GC: full experimental temperature range of Ref. [15]. Red (full) circles: experimental data points obtained from Ref. [15], using $\rho_c = 1113\,\mathrm{kg\,m^{-3}}$. Pink (full) curve labeled 1: Eq. (69), with $\rho_c = 1113\,\mathrm{kg\,m^{-3}}$ and a T_c shift of 0.5 mK. Pink (dotted) curve labeled 2: Eq. (69), with $\rho_c = 1113\,\mathrm{kg\,m^{-3}}$. Black (dotted) curve labeled GC_4: Eq. (69) from Ref. [15], with $\rho_{c,\rm GC} = 1110\,\mathrm{kg\,m^{-3}}$. Horizontal and vertical (pink) lines: from reference to the local value $\Gamma^+_{e,\rm cor} = 0.993 \times 0.07551466$ at $\Delta\tau^*_{\gamma_{e,\rm th}} = 4.347 \times 10^{-3}$ where $\gamma_{e,\rm th} = \gamma_{e,\rm fit} = 1.205879$ (see text). Horizontal blue line labeled $R\%\,(\Gamma^+_{e,\rm exact})$: residual for the "exact" local value $\Gamma^+_{e,\rm exact} = 0.0747481$ at $\Delta\tau^*_{\gamma_{e,\rm th}} = 4.347 \times 10^{-3}$ (see text); Other symbols, marks and labels: see text and previous figures.

Appendix B: EFFECTIVE POWER LAW ANALYSIS

An useful mathematical function to fit the isothermal compressibility data measured at finite distance to the critical temperature along the critical isochore is the simple power law:

$$\kappa^*_{T,\rm fit} = \Gamma^+_{e,\rm fit}\,(\Delta\tau^*)^{-\gamma_{e,\rm fit}}\,, \qquad \text{(B1)}$$

with an adjustable non-Ising exponent $\gamma_{e,\rm fit}$ and an adjustable effective amplitude $\Gamma^+_{e,\rm fit}$. The values of $\gamma_{e,\rm fit}$ and $\Gamma^+_{e,\rm fit}$ are then associated to the limited experimental temperature range $\Delta\tau^*_{\rm min} \le \Delta\tau^* \le \Delta\tau^*_{\rm max}$ of the fit. For example, Güttinger and Cannell have claimed that the correction to scaling terms are important by demonstrating in their Fig. 2 of Ref. [15], that their susceptibility measurements of high relative precision ($\sim \pm 0.2\%$) deviate systematically from a simple power law behavior with $\gamma_{e,\rm GC} = 1.206$ and $\Gamma^+_{e,\rm GC} = 0.6390\chi_{T,\rho}\,(\Delta\tau^*_{or})\,\frac{p_{c,\rm GC}\,(T_c)^{-1.206}}{(\rho_{c,\rm GC})^2} = 0.07867$. Looking in detail their figure, we note that $\gamma_{e,\rm GC} \simeq 1.206$ corresponds precisely to the slope of the tangent line to the experimental behavior close to the relative temperature distance $\Delta\tau^*_{\gamma_{e,\rm GC}=1.206} \simeq 4.35 \times 10^{-3}$, i.e., the local temperature value $T \simeq T_c + 1.25\,\mathrm{K}$ where we observe the extremum (around -4%) of the deviation curve. Hereafter, we have magnified this observation considering the isothermal compressibility data which account for our values of the critical density $\rho_c = 1113\,\mathrm{kg\,m^{-3}}$

and critical pressure $p_c = 5.84007\,\mathrm{MPa}$ in the equation $\kappa^*_{T,\mathrm{expt}} = \chi_{T,\rho,\mathrm{expt}} \frac{p_c}{(\rho_c)^2} \chi_{T,\rho}\left(\Delta\tau^*_{or}\right)$. Using Eq. (B1), we have then fitted the twelve data covering the restricted temperature range $9.115 \times 10^{-4} \leq \Delta\tau^* \leq 1.95 \times 10^{-2}$ (i.e., $0.26\,\mathrm{K} \leq T - T_c \leq 5.65\,\mathrm{K}$) defined by the segment labeled FIT and the gray area in Fig. 5 (see also the upper axis of Fig. 1). As expected, our fitting result

$$\kappa^*_{T,\mathrm{fit}} = 0.07551466\left(\Delta\tau^*\right)^{-1.205879}$$

is not affected by the increasing level of realistic uncertainties approaching T_c and shows excellent agreement with the Güttinger and Cannell's one (the amplitude difference accounts for about -4% correction noted above in this restricted temperature range). In Fig. 5, we have reported the residuals $\%R\left(\kappa^*_T\right) = 100\left(\frac{\kappa^*_{T,}}{\kappa^*_{T,\mathrm{fit}}} - 1\right)$ (expressed in %) for each experimental data point κ^*_T. In the fitting temperature range, the data dispersion is lowered at the $\pm 1\%$ level. Then, our Fig. 5, may be seen similar to Fig. 2 of Ref. [15] with a -4% zero shift in the vertical axis and a magnification of the high relative precision ($\sim 0.2\%$) of the Guttinger and Cannell's measurements in the fitting temperature range. In addition the mean (geometrical) value $\langle\Delta\tau^*_{\mathrm{fit}}\rangle = \sqrt{\Delta\tau^*_{\min}\Delta\tau^*_{\max}} = 4.215\times10^{-3}$ of our selected temperature range is very close to the temperature value of the extremum of the residuals (see below). For easy link with our previous figures, the lower and upper horizontal axes are labeled in a similar manner.

Since our fitting temperature range includes the value $\langle\Delta\tau^*_{or}\rangle = 4.215\times10^{-3}$, it is now essential to show that the uncertainty of the amplitude value $\Gamma_{e,\mathrm{fit}} = 0.07551466$ remains only related to the error-bar ($\sim\pm1.5\%$) on the calibration of the susceptibility data and the critical density value. We have then estimated the residuals for three different fitting results, using Eq. (69) with $\gamma = 1.241$, $\Delta = 0.496$, and the following set of parameters (i) $\Gamma^+ = 0.0577$, $a^+_{1\chi} = 1.29$, $a^+_{2\chi} = -1.59$, and $a^+_{3\chi} = 1.9$, i.e., the fitting parameters obtained by Güttinger and Cannell with $\rho_{c,\mathrm{GC}} = 1110\,\mathrm{kg\,m^{-3}}$, which leads to the dotted black curve labeled GC_4 in Fig. 5; (ii) $\Gamma^+ = 0.0577\left(\frac{\rho_c}{\rho_{c,\mathrm{GC}}}\right)^2$ and same values of $a^+_{1\chi} = 1.29$, $a^+_{2\chi} = -1.59$, and $a^+_{3\chi} = 1.9$, leading to the full red curve labeled 1 which account for the present critical density value; (iii) the latter parameter set and a shift of 0.5 mK in T_c, illustrated by the dotted pink curve labeled 2, which accounts for the realistic increase of the experimental uncertainty near T_c. The relative differences between curves 1 and 2 increases approaching the critical temperature, a result well-observed outside our temperature fitting range. The shape differences between curves 1 and GC_4 combine the effects due to a difference on the critical density values and a shift of 0.5 mK in T_c. *Finally, the well-defined extremum of the deviation curves in Fig. 5 is the most important consequence of the high relative precision of the Güttinger and Cannell's measurements.* That demonstrates that a well-defined local value (here $\gamma_{e,\mathrm{fit}} = 1.205879$) of the effective exponent can be measured at a well-defined local value of the temperature distance to T_c (here $\simeq T_c + 1.25\,\mathrm{K}$).

Now, we can refine the above power law analysis at finite distance to T_c, accounting thus for the theoretical effective behavior $\mathbb{Z}^+_{\chi,e}\left(\gamma_{e,\mathrm{th}}\right)$ illustrated in Fig. 2, with $\gamma_{e,\mathrm{th}}\left(t\right)$ and $\mathbb{Z}^+_{\chi,e}\left(t\right)$ defined by Eqs. (65) and (66), respectively. The condition $\gamma_{e,\mathrm{th}} = \gamma_{e,\mathrm{fit}} = 1.205879$ is observed at $t_{\gamma_{e,\mathrm{th}}=1.205879} = 9.159\times10^{-5}$, while the corresponding value of the effective theoretical amplitude is $\mathbb{Z}^+_{\chi,\gamma_{e,\mathrm{th}}} = 0.396926$. Using then $t = \vartheta\Delta\tau^*$ [Eq. (25)] and the asymptotic Ising-like value $\vartheta = 0.0211752$ defined in §2, we expect that the local value of the effective exponent must be observed at $\Delta\tau^*_{\gamma_{e,\mathrm{th}}=1.205879} = 4.347\times10^{-3}$ (i.e., $T - T_c \simeq +1.26\,\mathrm{K}$), in excellent agreement with the reduced temperature position of the extremum of the curve 1 in Fig. 5. From $\Gamma^+_{\gamma_{e,\mathrm{th}}} = \Gamma^+\vartheta^{\gamma-\gamma_{e,th}}\frac{\mathbb{Z}^+_{\chi,\gamma_{e,\mathrm{th}}}}{\left(\mathbb{Z}^+_\chi\right)^{-1}}$ [see Eq. (76)] where we introduce the asymptotic Ising-like values $\left(\mathbb{Z}^+_\chi\right)^{-1} = 0.269571$, $\Gamma^+ = 0.057824$ previously defined in § 2, the corresponding local value of the effective amplitude is $\Gamma^+_{\gamma_{e,\mathrm{th}}=1.205879} = 0.0747481$, i.e., a value only $\sim 1\%$ lower than $\Gamma^+_{e,\mathrm{fit}}$. However, when the effective power law of Eq. (B1) is directly use to obtain the corresponding local value, hereafter noted $\vartheta_{e,\mathrm{fit}}$, of the scale factor, we must underline the combined effects of the temperature distance, here accounted for by the exponent difference $\gamma - \gamma_{e,\mathrm{fit}} = 0.0337145$, and the experimental uncertainty, here attached to the amplitude value $\Gamma_{e,\mathrm{fit}} = 0.07551466$. Rewriting then Eq. (77) in the following form

$$\vartheta_{e,\mathrm{fit}} = \left[\frac{\left(\mathbb{Z}^+_\chi\right)^{-1}}{\mathbb{Z}^+_{\chi,\gamma_{e,th}}} \times \frac{\Gamma^+_{e,\mathrm{fit}}}{\Gamma^+}\right]^{\frac{1}{\gamma-\gamma_{e,\mathrm{fit}}}} \tag{B2}$$

we obtain $\vartheta_{e,\mathrm{fit}} = 0.028466$, i.e., a value $\sim 35\%$ higher than our asymptotic value $\vartheta = 0.0211752$. Such important discrepancy needs to complement our understanding of the role of the experimental uncertainty on $\Gamma^+_{e,\mathrm{fit}}$ in the determination of $\vartheta_{e,\mathrm{fit}}$, thanks to the high relative precision of the light scattering experiment of Güttinger and Cannell.

Indeed, a fitting procedure where the effective exponent and amplitude are free in minimizing the mean deviations over a *finite* temperature range is uncorrect. It must be replaced by a *local* envelope representation of the $\kappa^*_T\left(\Delta\tau^*\right)$-curve when the contribution (which continously increases with $\Delta\tau^*$) of the confluent corrections to scaling is only characterized by a single parameter. As a practical result, the fitting value $\Gamma^+_{e,\mathrm{fit}}$ of the effective amplitude is such as $\Gamma^+_{e,\mathrm{fit}} \neq \Gamma^+_{\gamma_{e,\mathrm{th}}=\gamma_{e,\mathrm{fit}}}$. For example, looking now at the 0.2% deviation level reported in Fig. 5, we can observe that the true tangent (pink) line of slope $\gamma_{e,\mathrm{fit}} = 1.205879$ has effectively an amplitude $\sim 0.7\%$ lower than the amplitude $\Gamma^+_{e,\mathrm{fit}}$ used as a reference. More generally, from Eq. (B2) and a careful analysis of the fit deviation curve to estimate $\delta\Gamma_{e,\mathrm{fit}}$ at the extremum po-

sition, we can write $\Gamma^+_{e,\rm cor} = \Gamma^+_{e,\rm fit}\,(1+\delta\Gamma_{e,\rm fit})$ and define the corrected value $\vartheta_{e,\rm cor}$ related to the local envelope by the equation

$$\vartheta_{e,\rm cor} = \vartheta_{e,\rm fit}\left(\frac{\Gamma^+_{e,\rm cor}}{\Gamma^+_{e,\rm fit}}\right)^{\frac{1}{\gamma-\gamma_{e,\rm fit}}} \simeq \vartheta_{e,\rm fit}\left(1+\frac{\delta\Gamma_{e,\rm fit}}{\gamma-\gamma_{e,\rm fit}}\right) \tag{B3}$$

From the Güttinger and Cannell's results of Fig. 5 where $\delta\Gamma_{e,\rm fit} \simeq -0.007$ and $\vartheta_{e,\rm fit} \simeq 0.028466$, we obtain $\vartheta_{e,\rm cor} \simeq 0.022556$ which is now in better agreement (+6.5%) with our asymptotic value $\vartheta \simeq 0.211752$. As previously underlined, *the precise description by a local exponent value defining the slope of the tangent line to the singular behavior of the isothermal compressibility of xenon at a well-defined temperature distance to T_c, is one major point of interest of the Güttinger and Cannell's results to validate the one-parameter crossover modelling predicted by the massive renormalization scheme.* Moreover, as indicated by the horizontal blue line corresponding to the residual $100\left(\frac{\Gamma^+_{\gamma_{e,\rm th}=1.205879}}{\Gamma^+_{e,\rm fit}}-1\right) = -1.015$, the expected value, at $\Delta\tau^*_{\gamma_{e,\rm th}=1.205879} = 4.347\times10^{-3}$, of the extremum which corresponds to the asymptotic value $\vartheta \simeq 0.211752$, is well compatible with the realistic experimental uncertainty.

Since the Güttinger and Cannell's results of highly relative precision $\lesssim 0.2\%$ have illustrated the significant role of the exponent difference $\gamma-\gamma_e$ when the restricted temperature range is selected outside the Ising-like preasymptotic domain, we can also estimate the related temperature effect of the uncertainty level on the value of ϑ (as calculated in Section 2). We consider thus an effective fitting procedure which provides the values of γ_e, Γ^+_e, and $\Delta\tau^*_e$, where it is assumed that the effective amplitude Γ^+_e is determined with a relative error-value $\delta\Gamma_e$, such as $\Gamma^+_{e,\rm exact} = \Gamma^+_e\,(1+\delta\Gamma_e)$. Here $\Gamma^+_{e,\rm exact}$ is *de facto* the exact value when it is defined such that

$$\vartheta = \left[\frac{\left(\mathbb{Z}^+_\chi\right)^{-1}}{\mathbb{Z}^+_{\chi,e}}\times\frac{\Gamma^+_{e,\rm exact}}{\Gamma^+}\right]^{\frac{1}{\gamma-\gamma_e}} \tag{B4}$$

In Eq. (B4), the value of $\mathbb{Z}^+_\chi$, Γ^+, $\gamma_{e,\rm th}\equiv\gamma_e$, and $\mathbb{Z}^+_{\chi,e}\left(\gamma_{e,\rm th}\right)$ are known with zero uncertainty from the mean crossover function for the susceptibility case. Using then Eq. (B1) and (B4), we obtain

$$\vartheta_e = \vartheta\left(\frac{1}{1+\delta\Gamma_e}\right)^{\frac{1}{\gamma-\gamma_e}} \tag{B5}$$

For each value $\gamma_e=\gamma_{e,\rm th}$ estimated at $\Delta\tau^*_{\gamma_{e,\rm th}=\gamma_e} = \frac{t_{\gamma_{e,\rm th}}}{\vartheta}$ with $\vartheta = 0.0211752$, we can easily calculate the isocline $\vartheta_{e,\delta\Gamma_e}\left(\Delta\tau^*_{\gamma_{e,\rm th}=\gamma_e}\right)$ at constant (small) value of $\delta\Gamma_e$, using the following approximation

$$\vartheta_{e,\delta\Gamma_e}\left(\Delta\tau^*_{\gamma_{e,\rm th}=\gamma_e}\right) \simeq \vartheta\left[1-\frac{\delta\Gamma_e}{\gamma-\gamma_e}\right] \tag{B6}$$

The corresponding isocline of the residuals is thus

$$r\%(\vartheta_{e,\delta\Gamma_e}) = 100\left(\frac{\vartheta_{e,\delta\Gamma_e}}{\vartheta}-1\right) = -\frac{\delta\Gamma_e}{\gamma-\gamma_e} \tag{B7}$$

Two pairs of symmetrical isoclines of Eq. (B7) are illustrated in Fig. 4(c) for $\delta\Gamma_e=\pm0.2\%$ (the relative precision of Güttinger and Cannell's data) and $\delta\Gamma_e=\pm0.02\%$, respectively, thus evidencing the experimental challenge to validate the equation $\vartheta = Y_c\left(\frac{\mathcal{Z}^{+,1}_\chi}{\mathbb{Z}^{+,1}_\chi}\right)^{\frac{1}{\Delta}}$ at the %-level when $\Delta\tau^*\lesssim10^{-3}$. The needs for a "critical" increase of the experimental precision when $\Delta\tau^*$ decreases is now well quantified by Eq. (B7) when the objective is to test the asymptotic validity of linearized Eqs. (60) or (61).

[1] M. A. Anisimov and J. V. Sengers, in *Equations of State for Fluids and Fluid Mixtures*, Part I, J.V. Sengers, R.F. Kayser, C.J. Peters, and H.J. White, Jr., Eds. (Elsevier, Amsterdam, UK, 2000) pp. 381-434.

[2] see for example Zinn Justin, *Euclidean Field Theory and Critical Phenomena* , 3^{rd} ed. (Oxford University Press, 1996).

[3] C. Bagnuls and C. Bervillier, J. Phys. (Paris) Lett., **45**, L-95 (1984).

[4] see for example C. Bagnuls and C. Bervillier, Phys. Rev. E **65**, 066132 (2002) and references therein.

[5] R. Guida and J. Zinn-Justin, J. Phys. A: Math. Gen. **31**, 8103 (1998).

[6] K. G. Wilson and J. Kogut, Phys. Rep. **12 C**, 75 (1974).

[7] V. Privman, P. C. Hohenberg, and A. Aharony, Universal critical point amplitude relations, in "*Phase Transitions and Critical Phenomena*", Vol. 14, Ed. C. Domb and J. B. Lebowitz (Academic Press, New York, 1991).

[8] F. J. Wegner, Phys Rev. B **5**, 4529 (1972).

[9] Y. Garrabos and C. Bervillier, Phys. Rev. E **74**, 021113 (2006).

[10] Y. Garrabos, C. Lecoutre-Chabot, F. Palencia, B. Le Neindre, and C. J. Erkey, Phys. Rev. E. **77**, 021116 (2008).

[11] R. J. Hocken and M. R. Moldover, Phys. Rev. Lett. **37**, 29 (1976).

[12] J. V. Sengers and M. R. Moldover, Phys. Lett. **66A**, 44 (1978).

[13] C. Bagnuls, C. Bervillier, and Y. Garrabos, J. Phys. (Paris) Lett. **45**, L-127 (1984).

[14] J. S. Kouvel and M. E. Fisher, Phys. Rev. **136**, A 1626 (1964).

[15] H. Güttinger and D. S. Cannell, Phys. Rev. A **24**, 3188 (1981).

[16] U. Närger and D. A. Balzarini, Phys. Rev. B **42**, 6651 (1990).

[17] Y. Garrabos, Ph. D. Thesis, University of Paris (1982).

[18] Y. Garrabos, J. Phys. (Paris) **46**, 281 (1985) [for an english version see e-print/cond-mat/0512408].

[19] Y. Garrabos, J. Phys. (Paris) **47**, 197 (1986).

[20] J. M. H. Levelt Sengers, W. L. Greer, and J. V. Sengers, J. Phys. Chem. Ref. Data **5**, 1 (1976).

[21] J. M. H. Levelt Sengers and J. V. Sengers, in "Progress in Liquid Physics", Ed. C. A. Croxton (John Wiley & Sons, New York, 1978) pp. 103.

[22] In this approach of scaling, we use the correlation length and the susceptibility as independent properties in terms of the two-scale-factor universality. We can then ignore the universal features related to the additive universal constant of the heat capacity. Moreover, in a pure fluid case, the critical background constant is mixed with the non-universal contribution of the regular background terms.

[23] Y. Garrabos, Phys. Rev. E **73**, 056110 (2006).

[24] Y. Garrabos and C. Lecoutre, preprint (2009), see hal-00363233.

[25] R. F. Berg, M. R. Moldover, and G. A. Zimmerli, Phys. Rev. E **60**, 4079 (1999).

[26] K. A. Gillis, I. I. Shinder, and M. R. Moldover, Phys. Rev. E **70**, 021201 (2004).

[27] K. A. Gillis, I. I. Shinder, and M. R. Moldover, Phys. Rev. E **72**, 051201 (2005).

[28] Y. Garrabos, F. Palencia, C. Lecoutre-Chabot, C. J. Erkey, and B. Le Neindre, Phys. Rev. E **73**, 026125 (2006).

[29] The entropy per particle $s_{\bar{p}}$ is related to the temperature derivatives $\gamma^{'} = \left(\frac{\partial p}{\partial T}\right)_{v_{\bar{p}}}$ and $\delta^{'} = \left(\frac{\partial \mu_{\bar{p}}}{\partial T}\right)_{v_{\bar{p}}}$, which, at the critical point, leads to the following dimensionless equation $s^*_{\bar{p},c} = Z_c\,(Y_c + 1) - x^*_{\bar{p},c}$, where $s^*_{\bar{p},c} = \frac{s_{\bar{p},c}}{k_B}$ and $x^*_{\bar{p},c} = \frac{\delta^{'}_c}{k_B}$ [see also Y. Garrabos, arXiv: cond-mat/0601088 (unpublished)].

[30] J. C. Le Guillou and J. Zinn-Justin, Phys. Rev. Lett. **39**, 95 (1977).

[31] J. M. H. Levelt Sengers and J. V. Sengers, Phys. Rev. A **12**, 2622 (1975).

[32] Y. Garrabos, B. Le Neindre, R. Wunenburger, C. Lecoutre-Chabot, and D. Beysens, Int. J. Thermophys. **23**, 997 (2002).

[33] Y. Garrabos, C. Lecoutre-Chabot, F. Palencia, D. Brosetta, B. Le Neindre, and C. J. Erkey, Phys. Rev. E **75**, 061112 (2007).

[34] Y. Garrabos, C. Lecoutre-Chabot, F. Palencia, D. Brosetta, B. Le Neindre, and C. J. Erkey, Phys. Rev. E **76**, 061109 (2007).

[35] H. W. Habgood and W. G. Schneider, Can. J. Chem. **32**, 98 (1954); **32**, 164 (1954).

[36] M. A. Weinberger and W. G. Schneider, Can. J. Chem. **30**, 422 (1952); **30**, 847 (1952).

[37] D. S. Cannell and G. B. Benedek, Phys. Rev. Lett. **25**, 1157 (1970).

[38] I. W. Smith, M. Giglio, and G. B. Benedek, Phys. Rev. Lett. **27**, 1556 (1971).

[39] V. G. Baidakov, A. M. Rubshtein, V. R. Pomortsev, and I. J. Sulla, Phys. Lett. A **131**, 119 (1988).

[40] V. G. Baidakov, A. M. Rubshtein, and V. R. Pomortsev, Fluid Mech. Res. **21**, 89 (1992).

[41] Y. Garrabos, C. Lecoutre, and F. Palencia, arXiv: 0707.3889 (unpublished).

[42] A. B. Cornfeld and H. Y. Carr, Phys. Rev. Lett. **29**, 28 (1972); **29**, E320 (1972).

[43] D. Balzarini and O. G. Mouritsen, Phys. Rev. A **28**, 3515 (1983).

[44] A. Michels, T. Wassenaar, and P. Louwerse, Physica **20**, 99 (1954).

[45] M. S. Green, M. Vicentini-Missoni, and J. M. H. Levelt Sengers, Phys. Rev. Lett. **18**, 1113 (1967).

[46] L. R. Wilcox and D. Balzarini, J. Chem. Phys. **48**, 753 (1968).

[47] M. Vicentini-Missoni, J. M. H. Levelt Sengers, and M. S. Green, J. Res. Natl. Bur. Stand. (U.S.) **73A**, 563 (1969).

[48] J. T. Ho and J. D. Lister, Phys. Rev. B **2**, 4523 (1970).

[49] W. T. Estler, R. Hocken, T. Charlton, and L. R. Wilcox, Phys. Rev. A **12**, 2118 (1975).

[50] P. C. Hohenberg and M. Barmatz, Phys. Rev. A 6, 289 (1972).

[51] H. L. Swinney and D. L. Henry, Phys. Rev. A **8**, 2566 (1973).

[52] R. F. Berg and M. R. Moldover, J. Chem. Phys. **93**, 1926 (1990).

[53] M. R. Moldover, J. V. Sengers, R. W. Gammon, and R. J. Hocken, Rev. Mod. Phys. **51**, 79 (1979).

[54] R. F. Berg, M. J. Lyell, G. B. McFadden, and R.G. Rehm, Phys. Fluids **8**, 1464 (1996).

[55] M. E. Fisher, S.-Y. Zinn, and P. J. Hupton, Phys. Rev. B **59**, 14533 (1999).